June 2021

Transparent Planar Micro-Electrode Array for In-Vitro Electric Field Mediated Gene Delivery

Raj Himatlal Shah
University of South Florida

Transparent Planar Micro-Electrode Array for In-Vitro Electric Field Mediated Gene Delivery

by

Raj Himatlal Shah

A thesis submitted in partial fulfillment
of the requirements for the degree of
Master of Science in Electrical Engineering
Department of Electrical Engineering
College of Engineering
University of South Florida

Major Professor: Andrew M. Hoff, Ph.D.
Mark J. Jaroszeski, Ph.D.
Stephen E. Saddow, Ph.D.

Date of Approval:
June 23, 2021

Keywords: ITO, Transparent Microelectrode, Low voltage electroporation

Dedication

I dedicate all my work to my professor, Dr. Andrew Hoff, and my family.

Acknowledgments

I would like to sincerely thank my professor, Dr. Andrew Hoff, who believed that I could complete this work. He was always a constant source of inspiration to me with the vast knowledge and would express my deepest gratitude for his time and the knowledge he shared. I heartfully thank my professor for letting me complete my thesis for no pressure and for guiding, motivating, supporting, and helping me in all ways to progress with the degree. And I would never think of another professor to guide me with my thesis.

I would also like to thank my committee professors, Dr. Mark Jaroszeski and Dr. Stephen E. Saddow, for their valuable time. I would also like to thank my colleagues, Alex Otten and Molly Skinner, for their helpful and precious support throughout my thesis.

And finally, I thank my mother, Jayna Himatlal Shah, my dad Himatlal Chhotalal Shah, my sister Darshita Himatlal Shah for their unconditional love, encouragement, and support that motivated me to gain a master's degree.

Table of Contents

List of Tables

List of Figures

Abstract

Gene delivery is the process of delivering the modified gene into the human cell. There are two types of gene delivery depending on where the target cells are. The in-vivo gene delivery deals with delivering the altered genes into the cells while still in the host body. While another approach is to extract the cells from the host body, transfer the modified gene into cells and then put these cells back into the host body, this approach is called the ex-vivo method.

A vector is a carrier that carries the modified gene to the host cell or body. Hence, depending on how the gene was brought into the contact of cells, there are two different methods. In Viral vectors, the viruses are the carriers; the viruses carry the required gene to the target cells. Non-viral methods use different approaches to deliver the modified gene to the cell's body. One of the non-viral vectors is the Physical method. In this method, the altered gene is introduced into the required cell using physical methods. In the physical method, the cell membrane is counteracted by using physical force. Electroporation is one of the many physical methods. In this method, a sufficient electric field is applied to the cell, causing the walls of the cells to open. Thus, creating pores using an electric field, hence electroporation.

Different devices have been made to achieve electroporation efficiently and conveniently. These include the use of cuvette and many other researched devices. This document contributes to this field by giving a methodology to fabricate a transparent microelectrode array that can deliver the DNA.

The advantage of this electrode is that it is transparent; hence it may be used to see the electroporation process when it is happening. Another advantage of this electrode is that it is a microelectrode. This means that the voltages required to reach the transmembrane potential are low compared to conventional methods. Lower voltage means less chance of cells dying during the process, increasing the efficacy of the process. Hence, higher electric fields can be attained with comparatively low voltages.

Chapter 1: Introduction

1.1 Gene Therapy

Since the recognition that gene is the basic unit of heredity, the objective of medical science is to make modifications in specific sites of the cell. In 1970, a research study enabled scientists to separate specific genes from a predetermined site in the DNA molecule and reinsert it in a reproducible manner [1]. Gene therapy, in simple terms, can be defined as the process of genetic modification of cells to result in a therapeutic effect [2]. These genetic modifications can be done in somatic cells or germline cells [1].

Somatic cell gene therapy is a type of gene therapy in which the normal gene is inserted into the somatic cells of the host [3]. Somatic cells are any cells in the body other than the reproductive cells such as sperm and egg cells [4]. This type of therapy involves curing the patient's disease and not the patient's descendant [3]. On the other hand, Germline cell therapy deals with inserting a normal gene into the germ cells: the sperm and egg cells of the parent or the early embryo of the offspring. In this type of cell therapy, the goal is to cure or change the child's gene and not the parent. Hence, if the parents suffer from a disease, their offspring will not inherit after this therapy [3].

There are two approaches to gene therapy; these two approaches are in-vivo gene therapy and ex-vivo gene therapy [2, 5]. The in-vivo approach deals with inserting the genes directly into the cell, which is in the living being. The advantage of the in-vivo approach is that it is less complex to carry out when compared to the ex-vivo approach. However, the targeting is not very specific,

and also the transfection is lower than the ex-vivo gene transfer [5]. Whereas in the ex-vivo approach, the cells are extracted from the living organism, followed by in-vitro culture and expansion, then followed by genetic modification, and then the cells are implanted back in the tissue of the living organism. Compared to the in-vivo approach, ex-vivo approach is laborious and expensive, but it can be used to selectively manipulate the desired cell type [5].

1.2 Delivery Methods in Gene Delivery

One of the critical challenges in gene therapy is the delivery methods: how the modified gene is delivered to the intended cell in the host's body. For this purpose, a carrier module referred as the vector is used to deliver the modified cells. The vector needs to specify a particular set of requirements for effective gene delivery; an ideal vector needs to be unrecognized by the immune system, capable of delivering one or more with different sizes that are required for clinical trials. The vector should not cause any reaction to the host's body once it is inserted [6]. Finally, it should express the gene for as long as it is required, generally the patient's lifetime [6].

Chapter 2: Viral Vectors

In Viral vectors, *"Harmless Viruses"* are used as vectors for transmitting the modified genes into the host's body. Viruses have evolved to encapsulate a particular gene and then deliver them to the human cells in a manner that then causes diseases. Scientists have tried to use this capability to their advantage by changing the virus's genes and replacing them with the working human gene. Then this virus delivers a healthy gene rather than a disease-causing viral gene. Some viruses insert their genes into the cells without entering the cells, while some viruses enter the cell membrane by disguising themselves as protein molecules. Once the virus reaches the desired location, the gene can be *"switched on"* to give instructions to the cell to produce the protein that the cell typically cannot build [6]. A few of the different types of viruses used in gene therapy are:

2.1 Retrovirus

These are the first virus vectors to be used in gene delivery experiments. They belong to a class of viruses that can create a double-stranded DNA copy using the enzyme called "reverse transcriptase." These copies of the DNA can then be integrated into host cell chromosomes by another enzyme of this virus known as "integrase" When these modified cells divide, the divided cells then have these new genes. Although this virus has been used in gene therapy experiments, they have a few problems. One such issue is that the integrase enzyme can insert the genetic material of the virus into any random position in the host's genome, this can lead to *"insertional mutagenesis"* (which happens when the virus is inserted in the middle of the gene) or

"uncontrolled cell division" (which occurs when the virus is the one controlling the cell division) leading to cancer. These problems are being addressed by using *"zinc finger nuclease"* or including specific sequences like *"beta-globin locus control region"* to redirect the site of integration to a particular chromosome [6].

2.2 Adenovirus

In response to the problems caused by inserting the genes in the wrong sites of the cell, researchers have tried different viruses. Adenovirus is a virus that has a double-stranded DNA structure, which causes infection in the respiratory tract, intestines, and eye linings (causes the common cold). These Viruses infect the host cell by introducing their DNA into the host. The DNA on this virus is just left in the host cell's nucleus; the information in this DNA is then transcribed just like any other gene. The advantage of Adenovirus over the retrovirus is that it can infect a wider variety of cells, including the slower multiplying cells such as lung cells. However, the disadvantage of the Adenovirus is that it is more likely to be attacked by the Human Immune System [6].

2.3 Adeno-Associated Viruses [AAVs]

Adeno-associated Viruses are small viruses from the Parvovirus family and have a single-stranded DNA structure. One advantage of AAVs is that they can affect a wider range of cells, including dividing and non-dividing cells. AAVs can insert genetic material at a specific site on Chromosomes 19 with nearly a certainty of 100% [6]. It is believed that most people carry AAV that does not provoke immune system response and does not cause any disease.

Scientists have demonstrated the use of AAVs to correct genetic effects in animals [6]. Now, AAVs are used to treat hemophilia, muscle and eye diseases. The main drawback of this virus is that it is small; due to this, it can only carry two genes in its natural state. Hence the payload of AAVs is relatively limited. Also, since the virus is inserted directly into the host cell's DNA, it can produce unintentional genetic damages [6].

2.4 Herpes Simplex Virus [HSV]

HVS is a neurotrophic virus (A virus capable of infecting the nerve cells) that is mostly used for gene transfer in the nervous system. These viruses have relatively large genomes compared to other viruses, enabling scientists to deliver more than one DNA into the host cells. HSVs can infect a broad range of tissues, including the liver, pancreas, muscles, and nerve and lung cells [6]. The wild type of HSV-1 virus can infect neurons that are not rejected by the immune system. In humans, antibodies to HSV-1 are common. However, complications due to herpes infections are somewhat rare [6].

Chapter 3: Non-Viral Vectors

Viral vectors are good when it comes to deliver the modified genes, but because of their immunogenicity, oncogenicity, and the fact that they can carry a small size of the DNA restricts their applications. However, non-viral vectors are safe, cost-effective, and reproducible compared to viral vectors. Also, they do not represent any limit on the size of DNA. However, the main drawback of the non-viral system is that they have low transfection efficiency, although improvements in the transfection efficiency are made by using different strategies [7]. Non-viral vectors are DNA plasmids that are delivered to the specified cell as naked DNA or associated with various compounds such as liposomes, gelatin, or polyamine [8]. The most utilized non-viral vectors are summarized in the table below [7].

Table 1: List of non-viral vectors [7].

Category	System for gene delivery	Subsystems
Inorganic particles	Calcium Phosphate	
	Silica	
	Gold	
	Magnetic	

[1]

[1] Portions of this chapter have adapted from, "Non-Viral Delivery Systems in Gene Therapy", by Rodriguez, A., Del, A., Angeles, M., 2013, (doi:10.5772/52704). Under the Creative Commons Attribution License 3.0. Permission is posted in Appendix A.

Table 1(continued).

Synthetic or natural biodegradable particles	Cationic lipid-based non-viral vectors	Cationic liposomes
		Cationic emulsions
		Solid lipid nanoparticles
	Peptide-based non-viral vectors	Poly-L-lysine
		Other peptides to functionalize other delivery systems
	Polymeric-based non-viral vectors	Poly (lactic-co-glycolic acid) (PLGA)
		Polylactic acid (PLA)
		Poly (ethylene imine) (PEI)
		Chitosan
		Dendrimers
		Polymethacrylates
Physical methods	Needle injection	
	Ballistic DNA injection	
	Electroporation	
	Sonoporation	
	Photoporation	
	Magnetofection	
	Hydroporation	

3.1 Inorganic Particles

Inorganic nanoparticles are nanostructures of different sizes, shapes, and porosity. These nanoparticles can be modified in such a way that they can avoid the reticuloendothelial system [7]. The preparation process for inorganic particles is easy and also their properties and characteristics are easily enhanced using surface functionalization. They have good storage stability and are not susceptible to microbial attacks [7]. Silica, Gold, Calcium phosphate, and many other magnetic compounds are the most studied particles. Nanoparticles, coated with silica are biocompatible materials. Also, gold nanoparticles have been used lately in gene therapy. They have low toxicity; their surface can be modified with different chemical techniques, and they can be easily prepared [7].

3.2 Synthetic or Natural Biodegradable Particles

Synthetic or natural biodegradable particles can be composed of cationic polymers, cationic lipids, or cationic peptides and can be from combinations of these components [7]. The main advantage of these biodegradable carriers is their reduced toxicity, and since they degrade inside the body, this lowers the accumulation of polymers in the cells. Different types and subtypes of these particles are given in table 1 above [7].

3.3 Physical Methods for Gene Delivery

Researchers are now attracted to the physical methods for gene therapy as it is a more straightforward method [9]. In this method, a physical force is used to counteract the cell's membrane barrier, helping intracellular delivery of the genetic materials [9]. This genetic material is introduced directly into the cells without any particulate or viral system.[7]. Various physical methods for delivery are listed in table 1 above.

Chapter 4: Electroporation

One of the major problems in cancer chemotherapy and biotherapy is the absence of effective drug and gene delivery. Various non-viral methods have been suggested for drug and gene delivery, such as chemical and physical methods. Physical delivery methods are one of the efficient non-viral methods. These methods include electroporation, micro-injection, gene gun, tattooing, laser, and ultrasound [10].

4.1 Introduction

Electroporation (EP) is the process of the formation of aqueous pores in the lipid bilayers by applying short high-electric field pulses (with a duration of microseconds to milliseconds) to bypass the cell membrane barrier. This transient permeable state can be used to transfer various molecules, including ions, drugs, dyes, antibodies, RNA, DNA, and tracers in the cells [11]. Electroporation is used to direct DNA vaccines against various infectious diseases such as influenza, HIV, Hepatitis C, malaria, and anthrax, increasing the immune response or treating or preventing tumor development, including prostate cancer and breast cancer, and melanoma [12]. For both in-vivo and in-vitro and in-patients, drug delivery to malignant tumors using electroporation has been proven beneficial [10]. Studies show that vaccines administrated using electroporation are safe and have an effective modality for the treatment of prostate cancer [10]. Data also suggest that electroporation of DNA vaccines in-vivo is an effective method to increase the cellular DNA uptake and gene expression in tissues, which leads to significant improvements

in the response of the immune system. Electroporation represents a way of increasing the number of DNA-transfected cells and intensifying the magnitude of the gene expression with reduced inter-subject variability requiring less time to reach the maximum immune response compared to conventional methods [13].

However, the use of electroporation results in the death of cells; this primarily happens when the electric fields cause permanent permeabilization of the cell membrane, followed by loss of cell homeostasis. This is called *"irreversible electroporation"* [14]. With little effort, electroporation can be improved. Moreover, electroporation increases the range of drugs delivered transdermally when used alone or with some enhancement methods [10]. The physicochemical properties of the drug and electrical parameters affect the efficacy of the transport. High-voltage pulses are well tolerated for in-vivo applications, but muscle contraction is induced [10]. It was shown that the addition of poloxamer188, before or immediately after the electroporation increases the number of reversible electro-pores through which the chemicals are administered into the cells [10]. It is seen that electroporation achieved through low voltages can induce immunity and protect mice cells effectively [10].

4.2 Theoretical Consideration in Electroporation

Different effects are experienced by cells when they are subjected to electric fields. Electrical perturbations cause scalar as well as vector effects on the cells. Electro-mechanical effects such as stretching and deformation lead to *"Joule heating"* [11]. The transmembrane potential $\Delta\Psi_E$ of a cell is given by the formula below [15]: -

$$\Delta\Psi_E = \Psi_{in} - \Psi_{out}$$

For spherical cells, the induced transmembrane potential is given as [15]: -

$$\Delta\Psi_E = \frac{3}{2} * E * r * Cos(\theta)$$

In the above equation, the letter E denotes the electric field generated, r denotes the radius of the cell, and θ denotes the angle between the normal to the cell surface and the direction of the electric field. In the above formula, the fraction 3/2 is because of the cell geometry. For spherical cells, the value is 1.5, for other geometry, the value will be different.

4.3 Method to Conduct an Experiment

Electroporation can be done in different ways depending upon the type of cells. Cells cultured on a Petri dish, removed from the culture media, can be placed in a buffer solution. This buffer solution limits the "*Joule effect*" and hence helps to preserve cell viability. This buffer comprises a combination of a 10mM phosphate buffer, a 250mM sucrose, and a 1mM $MgCl_2$. From a practical point of view, the bottom of the Petri-dish can act as an electro-pulsation chamber. For cells suspended in culture media, the cells can be separated from the culture medium by centrifugation, followed by resuspending them in the pulsing buffer.

After suspension in PBS, the cells can be placed in the cuvettes. A cuvette is nothing but a small tube-like vessel with a cross-section similar to a circle or a square. One end of it is sealed and it is made of a clear, transparent material such as plastic or glass. A set of electrodes is used to generate an electric field. This field is generated by supplying electric pulses from a pulse generator. A Square wave pulse generator is used in most experiments to control the pulse amplitude and pulse duration independently. This is important, especially in mammalian cells

where the outermost layer of the cell is just a delicate protein-embedded phospholipid layer [16]. Hence such structures are more affected by electric pulses than yeast and bacteria. The pulsing parameters need to be carefully selected depending on the type and geometry of the cell [17].

Chapter 5: Hypothesis and Research Aim

5.1 Introduction

Traditionally, electroporation of in-vitro cells is performed by cuvettes where the cells are suspended for applying electric pulses [18]. Notably, in the case of electroporation of adherent cells, a trypsinization protocol needs to be carried out. This protocol results in increased stress to the cells, affecting both the invasiveness of the operation and electroporation efficiency [19]. Other than this, there are several reasons to believe that in-situ electroporation is more suitable for achieving high-efficacy transfection in adherent cells while maintaining reasonable viability [20].

Electroporation methods using micro-chips are gaining interest because of their low consumption of cells and biomolecules and improved cell viability by reducing the cell damage induced due to high voltages compared to conventional cuvette-type electroporation systems [21]. And, unlike traditional electroporation, microchips enable electroporation of various cell types and molecules with high throughput, providing an ideal tool for gene function screening.[21-25].

These microfabricated electroporation chips allow reaching the high-intensity fields of 1 to 10kV/cm using very low voltages due to the reduced distance between the electrodes. For example, an electroporation chip was used to transfect the adherent cells using less than 2V successfully [26]. Also, the reduction in the required amplitude to create pores in the cell membrane reduces the cost and complexity of the pulse generator used in traditional electroporation systems and the devices' electrical safety [20]. It also minimizes the damage to the user in case of device malfunction.

5.2 Hypothesis and Research Aim

As mentioned in the introduction, there have been various successful attempts in making a micro-fabricated electroporation device. This research aims to develop a similar micro-fabricated electroporation device that results in higher transfection and reduced cell stress and operation at low voltage and current, thereby reducing cell death and improving cell viability after the electroporation procedure. Also, since lower voltages are used, there is no need for the bulky pulse generator, reducing the total cost of operation.

This research aims to design a similar micro-fabricated device for electroporation and gives the same advantages as those mentioned above. The intended Microfabricated device is made from a substrate of ITO (Indium Tin Oxide) on PET (Polyethylene terephthalate). ITO is a biocompatible material [27] that conducts current [28]; it serves as an ideal material for fabricating an interdigitated microelectrode structure. Also, because ITO is a transparent material, this micro-structure can be used to see the electroporation under the microscope and collect real-time data. Also, it can be used to see the effect on the cell membrane before, after, and during electroporation. Since ITO is a biocompatible material, this can be a first step towards the lab on chip concept where the cells are grown on the ITO electrode and then electroporated there itself. Various experiments and the procedure of the device fabrication are mentioned in the following chapter.

Chapter 6: Devices, Equipment, and Software

In this chapter, the devices, equipment, and software used to fabricate the microelectrode array on ITO are mentioned.

6.1 Analysis Tools

6.1.1 Inverted Microscope

Two inverted microscopes were used in this fabrication process. Leitz Wetzlar's Leica DM IL LED inverted microscope was used for counting cells and for viewing the transfected cells. Zeiss's Axiotron inverted microscope was used for measuring the dimensions of the micro-array. This microscope was used in conjunction with the BCAM viewer software for taking snapshots of the electrode. The measurements were done using the "Image J" software.

6.1.2 Power Supply

A 36 volts dual power supply was used as a power source for pulsing the micro-array. It was also used as a power source for current and voltage measurements while characterizing the silver contacts to the ITO.

6.1.3 Trypan Blue

Trypan blue stain (15250061, Life Technologies, Grand Island, New York) is a type of stain that turns blue when it interacts with the cell's intracellular protein, which means that the dead cells turn blue. The mechanism of trypan blue is that it is negatively charged, and it does not interact with the cells unless the cell membrane is compromised [29]. Trypan blue was used to identify and count the dead cells for calculating viability.

6.1.4 Sytox™ Green

Sytox™ Green Nucleic Acid Stain (S7020, Life Technologies, Eugene, Oregon) is a type of stain that glows when it comes in contact with the Nucleic acid inside the cell (which means that the cell glows in two cases, one if the cell is dead or if the stain has somehow penetrated inside the cell). Hence Sytox™ Green was used to determine the delivery of chemicals inside the cell, which justifies the working of the microelectrode array.

6.1.5 Multi-Meter

A multimeter was used for current and voltage measurement when characterizing the silver contacts to the ITO. Keithley's 2001 multimeter was used during the measurements. Following is the image of the multimeter used.

Figure 1: Keithley 2001 multimeter.

6.1.6 Arduino UNO

An Arduino Uno was used as a microcontroller to control the pulsing parameters. It is the heart of the pulsing circuit used to pulse the electrode.

6.1.7 Plate Counter

BioTek's FLx800 Microplate Fluorescence Reader (BT-FLX800T, BioTek, Winooski, VT) was used along with BioTek's Gen5 Data Collection and Analysis Software to analyze the fluorescence data. The following is the image of the plate reader used.

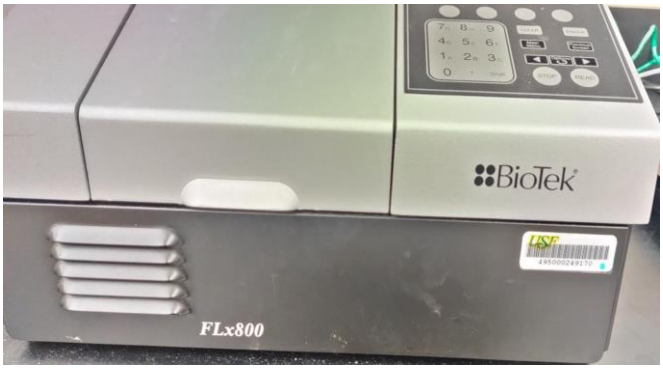

Figure 2: BioTek's FLx800 plater reader.

6.1.8 Haemocytometer

Hausser Scientific's Bright Line 3110 Haemocytometer was used for counting the alive and dead cells. The following is the image of the Haemocytometer used.

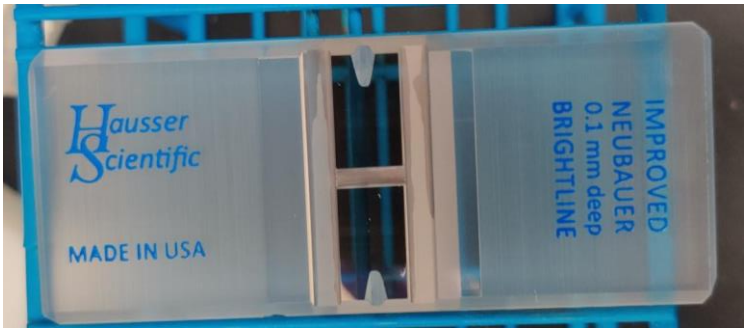

Figure 3: Hausser scientific's hemocytometer.

6.2 Fabrication Tools

The following sections talk about the tools that were used for fabricating the microelectrode array.

6.2.1 Spin Coater

Integrated Technologies, Inc's P-6000 spin coater was used to spin coat the ITO film with a positive photoresist.

6.2.2 Hot Plate

Two hot plates were used in the fabrication process. One was used for soft-bake the photoresist on ITO after application. Another hot plate was used to cure the silver epoxy on ITO, and a similar hot plate was used to heat Hydrochloric acid (HCL) and water solution when etching ITO.

6.2.3 Wet Bench

A wet bench was used for etching ITO, apply silver epoxy on the electrode, and for 2-part epoxy application. The wet bench was also used for rinsing the sample multiple times in the process of lithography.

6.2.4 DLP System

Intelligent micropatterning, LLC's SF-100 DLP system was used to print micro-array patterns on the photoresist coated ITO sample. The following is the image of the DLP system used.

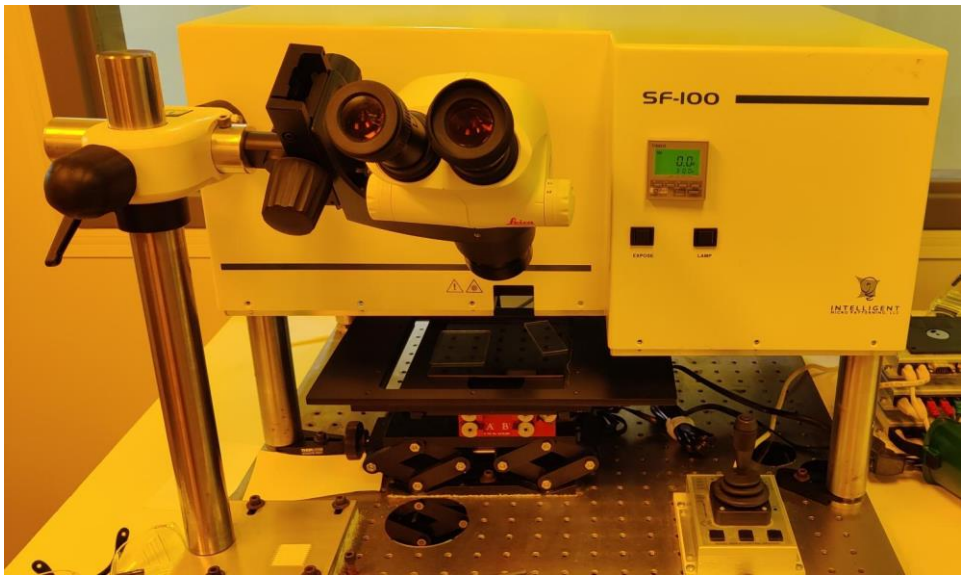

Figure 4: Intelligent micropatterning, LLC's SF-100 DLP system.

6.2.5 Paint Software

Microsoft paint software was used to design a bitmap image of the mask used to pattern the photoresist on the ITO sample.

6.2.6 Paper Knife

A paper knife was used to cut the ITO sheet into small samples for different experiments throughout the fabrication process. A 3-d printed hollow cylinder was used as a reference to cut the ITO sheet into near-circular samples.

6.2.7 ITO Sheet

"Thorlabs's OCF2520" ITO on PET sheet was used in different experiments done during the fabrication process of the microelectrode array. The front and backside of the ITO sheet were covered in a protective film, a transparent film on the ITO (top) side, and a blue film on the PET (back) side. The protective film was required to remove before doing any experiments on the ITO sheet. The following is the image of one sheet of ITO on PET from Thor labs. Figure 6 shows the cross-sectional view of the ITO sheet.

Figure 5: A sample ITO sheet on PET.

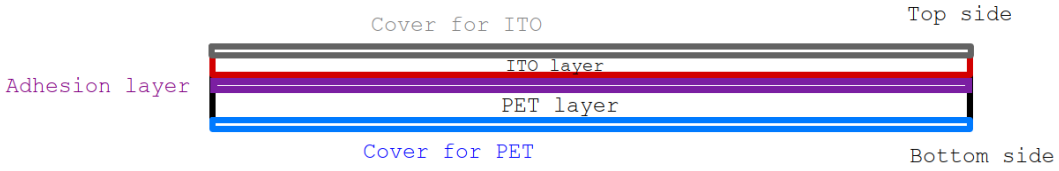

Figure 6: Cross-sectional view of the ITO sheet.

6.2.8 3-d Printer

A 3-d printer was used to print various objects used in the process of fabrication of the microelectrode array.

6.2.9 Copper Wires

Two single-stranded non-insulated copper wires were bonded to ITO to make contact with the Electrode. These copper wires were bonded to ITO using the MG chemical's 8331 S Silver epoxy.

6.2.10 2-Part Epoxy

Gorilla 2-part epoxy was used to passivate the exposed metallic parts on the electrode. The metal parts were the silver epoxy and the non-insulated copper wires. The epoxy was only applied to the lower parts for the copper wires that might contact the medium.

6.2.11 Soldering Station

A soldering station was used to put together the pulsing circuit, used to pulse the micro-array electrode to transfect the cells. The following is the image of the soldering station.

Figure 7: AOYUE int 968A Soldering station.

6.2.12 Silver Epoxy

MG chemical's 8331 S silver epoxy was used to bond copper wires to the ITO on PET. This epoxy comes in two parts which are then mixed in equal proportion before application. The epoxy is required to mix for more than 2 minutes before the application and is required to cure at 60°C for 60 mins of curing.

6.3 Cell Culturing Devices Tools

6.3.1 Cells

Jurkat, Clone E6-1 (ATCC® TIB-152™, American Type Culture Collection, Manassas, VA) cells were used in this research. The cells were used to test the biocompatibility of the ITO also for justifying the working microelectrode array.

6.3.2 Co_2 Cell Incubator

Thermo Fisher's HERAcell VIOS 160i Co_2 incubator was used to incubate the cells while doing the viability test of the ITO. It was also used to incubate the recultured cells for experiments on the micro-array Electrode.

6.3.3 Cell Media

Cell culture media was made by mixing RPMI 1640 with 1x L-glutamine (10040CV, Corning, Manassas, VA) with 10x Fetal Bovine Serum (Corning 35011CV, Corning Cellgro, New York, New York) and 1x Penicillin-Streptomycin (P4333, St. Luis, MO, USA).

6.3.4 6-Well Tissue Culture Plate

Sterile six-well tissue culture-treated plates (3516, Corning, Kennebunk, ME) were used to perform the viability test of the ITO and to perform the experiment with the Micro-electrode array. The electrode was placed inside one of the wells before experimenting. Also, the diameter of the well plate served as a reference diameter for the electrode array. The following is the figure of the culture plate used.

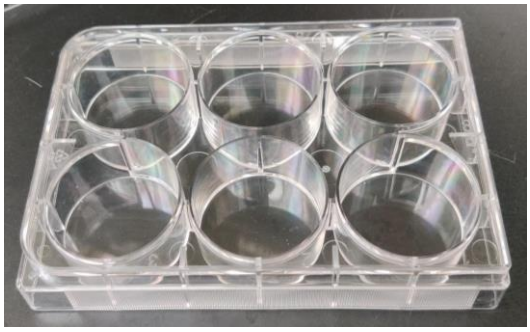

Figure 8: Corning's six-well tissue culture plate.

6.3.5 PBS

DPBS (Dulbecco's Phosphate Buffered Saline) (21-030-CV, Corning, Manassas, VA) was used to suspend the cells after removing them from the culture media. PBS was also used to characterize the pulse before starting experiments with the cells.

6.3.6 Centrifuge

Eppendorf's 5810 R centrifuge was used to separate the cells from the culture media and suspend them in PBS to achieve the desired concentration. The cells were centrifuged for 3 minutes at a speed of 150rpm to separate them from the media and suspend them in PBS. The following is the image of the centrifuge used.

Figure 9: Eppendorf's centrifuge.

6.3.7 Culturing Flask

Corning's canted neck 75cm^2 sterile Polystyrene flask (CLS 430641, Corning incorporated, NY) was used to culture and re-culture the cells during the whole period of the research. The flask was changed every four weeks after the first culture.

Chapter 7: Experiment, Results, and Conclusions

As mentioned in chapter 5, we introduced ITO as a suitable material for fabricating the microelectrode array. This chapter talks about the different experiments that were performed on the ITO. The experiments below are in a sequence showing the fabrication process starting from the ITO sheet to the final micro-electrode array.

7.1 Sheet Resistance Measurement

The micro-electrode is fabricated on the ITO sample shown in figure 10. Hence it is necessary to characterize the ITO sheet before proceeding further with the fabrication. The reason for this is that it is essential to make sure that the received product is the intended product. The first test is the sheet resistance test. The following was the procedure used to measure the sheet resistance of the bulk ITO sheet.

7.1.1 Procedure

For measuring the sheet resistance of the bulk ITO, the “Four-point probe test” was used. The following is the procedure used for measuring the sheet resistance of the ITO sample.

1. Cut the ITO sheet into a small sample. The sample should be approximately the same size as that of the diameter of the six-well plate tissue culture plate. The figure below shows

the sample used for measurement. (Note: in the figure below, the plastic coating on the sample is before the test.)

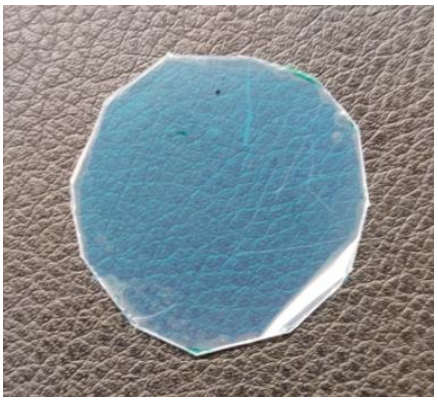

Figure 10: ITO sample used for sheet resistance measurement.

2. After the sample is ready, set up the four-point probe station.

3. After setting up the station, put the sample on the holder and turn on the vacuum.

4. Set the desired amount of supply current on the current source and measure the voltage on the multimeter.

Table 2 in the results section shows the voltage reading obtained for the respective input current. The four-point probe provides the resistivity (ρ) of the sample under test. After getting the resistivity, the following formula is used to calculate the sheet resistance.

$$Rsh = \frac{\rho}{t} \qquad (\Omega/\square)$$

The above equation is approximated to the formula shown below. This approximation is done considering the equipment used for the test [30]. This approximation is done for the condition

where the spacing between the probes (s) is very less compared to the thickness of the material (t) under test, in this case, the ITO sheet.

$$Rsh = \frac{\pi}{ln(2)} * \frac{Vm}{Is} \left(\frac{\Omega}{\square}\right) \ldots\ldots\ldots\ldots\ldots for\ s \ll t$$

In the equation below [30], *"Rsh"* is the sheet resistance, "*Vm"* is the measured voltage, *"t"* is the thickness of the ITO on PET, and "*Is"* is the supply current.

7.1.2 Results

The table below shows the measured voltage reading and corresponding calculated sheet resistance value.

Table 2: Measured values from sheet resistance test.

Sr. no	Supply current (µA)	Measured Voltage (mV)	Calculated sheet resistance (Ω/□)
1	100	10	453.236
2	10	1	453.236

No more than two readings were taken in this test since the sheet resistance value was consistent for both the reading. Also, the measured sheet resistance falls in the manufacturer's given range, which was between 350 to 500 ohms per square.

7.2 Thickness Measurement

A thickness measurement test was also performed on the sample to measure the thickness of the ITO on the PET sheet. Alpha step measurement was performed on the ITO sheet. For this

test, an etched ITO sample was required. The sample in the following figure was used to perform the test. The test was done on the patterned part in the figure below.

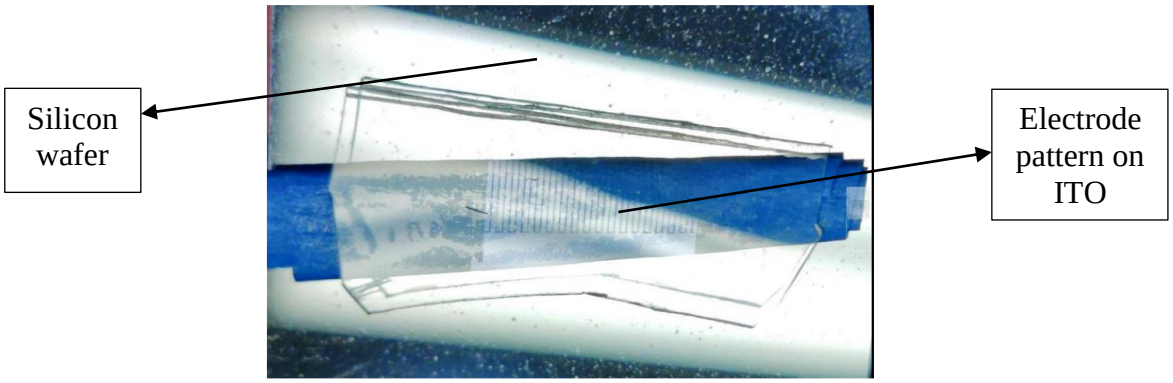

Figure 11: Etched ITO sample attached to the silicon wafer.

The sample used was etched for 3 minutes. And the resulting ITO thickness was in the range of 200 to 500 Angstroms, equal to 20 to 50 nm.

7.3 Biocompatibility Test

The final goal of the microelectrode array is to pulse the cells. Hence, it is necessary to know that if the material itself is harmful to the cells. In other words, it is required to make sure that the material that is used causes no damage to the cells. For this, it is necessary to test the biocompatibility of the material. Hence, a biocompatibility test is performed on the ITO. A biocompatibility test was also performed on the etched samples. The reason for this test was to evaluate the biocompatibility of the material that was left after ITO was etched. In the following subsection, the procedure and results achieved from both tests are mentioned.

7.3.1 Procedure

The ITO sheet was cut into small near-circular-shaped samples; the diameter of the cut circles was equal to the diameter of the 6-well tissue culture plate mentioned in the previous

chapter. These samples were cut with the help of a paper-knife and a 3d-printed hollow cylinder with its outer diameter equal to that of a tissue culture plate. A total of 6 samples were cut from the sheet to obtain the viability of the material. Jurkat, Clone E6-1 cells were cultured for 48 hours before the experiment in Corning's culturing flask in the CO_2 incubator. After culturing, the cells were at the concentration of 1.74 million cells per milliliter with a viability of 100%.

For performing the test, 6 ITO samples were put in the culture plate. After that 0.4ml of the cultured cells, and 3.6ml of cell media were placed on the top of each ITO sample. A total of 6 control samples were also formed by adding 0.4 ml of cells with 3.6 ml of cell media. Finally, the cells in control with ITO samples were recultured in a Co_2 incubator for 48 hours. After 48 hours, the cells were removed from the incubator, and the viability of the cells was assayed using the Trypan blue exclusion test [31].

For assaying the viability, 50uL of cells were mixed with 50uL of the trypan blue in 1:1 proportion; after that, the mixed solution was put into the hemocytometer and counted using the inverted microscope. Dead cells were recognized by a blue tint, while alive cells were recognized by the transparent circle with a black outline.

Finally, the viability of the cells was counted using the following formula stated in this document [31].

$$viable\ cells\ (\%) = \frac{total\ number\ of\ viable\ cells\ per\ ml\ of\ aliquot}{total\ number\ of\ cells\ per\ ml\ of\ aliquot}\ x\ 100$$

The same procedure was used to find the biocompatibility of the ITO after etching.

7.3.2 Result

The viability of 12 samples was calculated using the formula above, shown in table 3.

Table 3: Values obtained from control samples in biocompatibility test.

Control				
Sr. no	Number of alive cells	Number of dead cells	(%) Viability	Concentration (Millions/ml)
1	146	0	100	0.584
2	164	1	99.39	0.656
3	360	2	99.44	1.44
4	302	0	100	1.208
5	105	0	100	0.420
6	344	0	100	1.376
Average			99.805	0.9473

Table 4: Values obtained from the ITO sample in biocompatibility test.

ITO samples				
Sr. no	Number of alive cells	Number of dead cells	(%) Viability	Concentration (Millions/ml)
1	149	0	100	0.596
2	143	0	100	0.572
3	81	1	98.78	0.324
4	117	1	99.15	0.468
5	159	9	94.64	0.636
6	184	3	98.39	0.736
Average			98.66	0.5553

Table 5: Etched sample biocompatibility test data for control samples.

Control				
Sr. no	Number of alive cells	Number of dead cells	(%) Viability	Concentration (Millions/ml)
1	258	2	99.2	1.032
2	153	1	99.3	0.612
3	259	2	99.2	1.036
4	134	0	100	0.536
5	213	5	97.70	0.852
6	143	3	97.9	0.572
Average			98.88	0.7733

Table 6: Etched sample biocompatibility test data for etched samples.

Etched ITO samples				
Sr. no	Number of alive cells	Number of dead cells	(%) Viability	Concentration (Millions/ml)
1	195	0	100	0.780
2	291	1	99.65	1.164
3	301	2	99.33	1.204
4	148	3	98.01	0.592
5	226	0	100	0.904
6	213	1	99.5	0.852
Average			99.41	0.916

The viability of 12 samples is shown in table 3. Also, from Table 4, the average viability of the cells on the ITO is 98.66%, which implies that ITO is biologically compatible [27]. Also, from tables 5 and 6, it is clear that the viability of the cells on the etched ITO sample and control is above 95%. This means that both the ITO and the layer obtained after etching the ITO are biocompatible. Hence ITO on PET can be used as the base material for fabricating the microelectrode array.

7.4 Patterning ITO

After evaluating the viability of the ITO, the next step is to pattern the ITO. Patterning the ITO is the first step in the creation of the Planner Micro-electrode array. In this step, the ITO film is coated with a photosensitive material, and then the photosensitive material is patterned. The following subsection talks about the process in detail.

7.4.1 Procedure

After the ITO sheet is cut into small circular-shaped samples, the next step is to pattern the ITO. The patterning of the ITO is done similarly to that of patterning the silicon wafer. The process starts from spin coating the photosensitive material on the top of the circular ITO sample. “AZ1512

Positive photoresist" was used to spin coat using the spin coater to form a thin layer of positive photoresist on the top of ITO. Two-step coating was used to achieve a uniform coat of the photoresist on the sample.

In two-step coating, the sample is first rotated at low speed with a constant discharge of photoresist on the top of the sample; once the resist covers all the sample, then the speed is ramped up to 3000 rpm, and the sample is spun for 2 minutes resulting in a 1.39μm thick photoresist layer on the top of ITO sample [32]. After spin coating, the next step is to soft-bake the sample for ensuring proper adhesion of the resist to the ITO surface. The sample was soft-baked for 1 minute at 90°C.

After soft baking, the next step is patterning. For patterning, a mask shown in figure 12 was used. The mask in figure 12 was designed on "paint" software available in Microsoft windows, and the design specifications of the electrode mask used are listed in table 7.

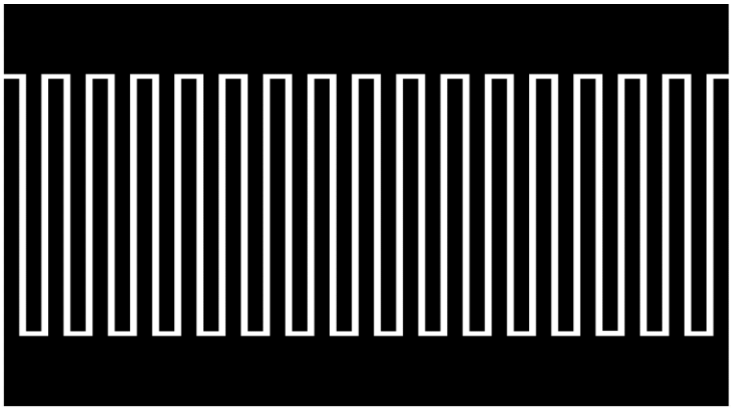

Figure 12: Image of the electrode mask used.

After the mask was ready, a DLP system was used to print that mask on the photoresist-coated ITO sample. For using the DLP system, first, the mask image needs to be opened on the connected computer; after that, the sample is aligned such that the beam focuses on the sample.

After that, the final step is to set the exposure time. For a 1.5µm thickness of photoresist, a 30 sec exposure time was used to pattern the photoresist coated on the ITO sample. After patterning, the sample was developed. “AZ 726 MIF” developer was used to develop the exposed photoresist. Figure 13 shows the image of the patterned and developed resist on the ITO sample.

Table 7: Design parameters for the electrode mask.

1 Pixel	15 Micrometres
Length of the mask	948 Pixels
Width of the mask	768 Pixels
Distance between the electrodes	9 pixels
Length of one electrode	491 pixels
Width of one electrode	20 pixels
Total number of electrodes	33
Number of electrodes in one side	17
Number of electrodes on another side	16
The total size of the mask with white areas	1024 x 768 pixels

As shown in figure 13, the left and right parts of the electrode are still covered in the resist. Hence the top and the bottom part of the electrode are still connected. Since the final aim of the device is to generate an electric field, the top and the bottom part of the electrode needs to be separated from.

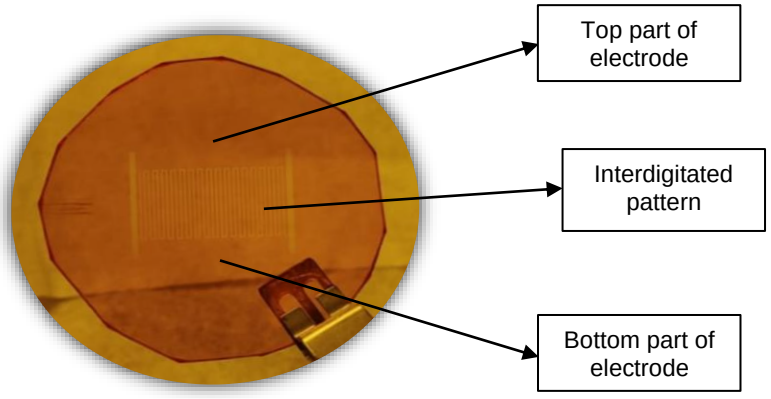

Figure 13: Figure of ITO sample with electrode pattern on it.

To isolate both the top and bottom parts of the electrode, photoresist on both the right and left parts near the electrode array were removed using “Cotton Q-tips.” To remove the photoresist, Q-tips were dipped in acetone and rubbed on the regions where the resist was required to remove. Figure 14 shows the modified sample with isolated top and bottom parts.

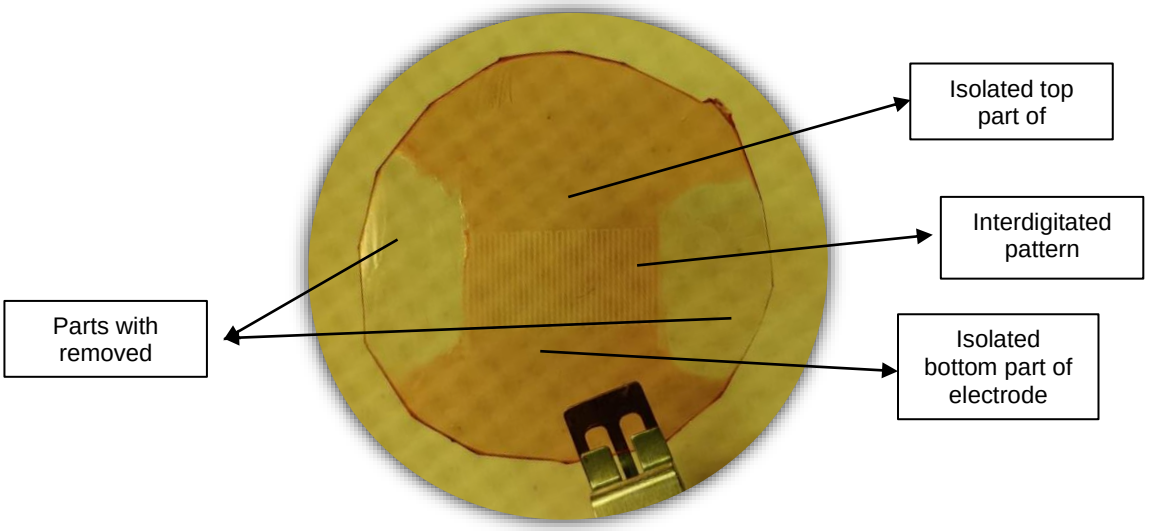

Figure 14: ITO sample with isolated top and bottom part.

7.4.2 Results

Figure 15 shows the microscopic images of the modified sample, and these images were taken to make sure that the top and the bottom parts of the electrode are separated from each other.

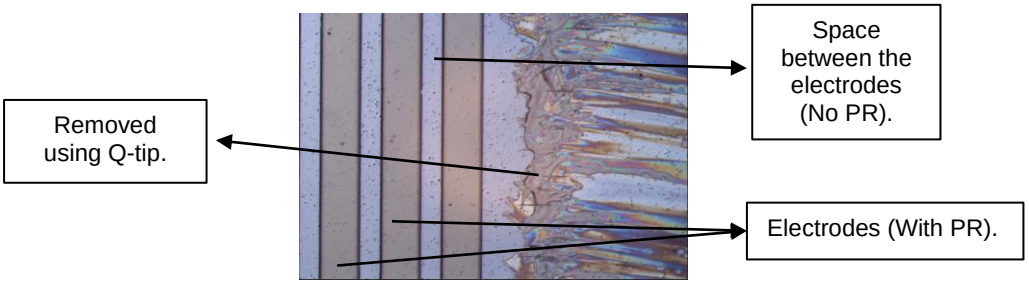

Figure 15: Edge of the electrode with 2.5x magnification.

7.5 Etching ITO

Once the photoresist is patterned, the next step is etching. A mixture of Hydrochloric acid and water was used for etching the ITO. The following subsection talks more about etching ITO.

7.5.1 Procedure

The procedure for etching was obtained by the trial-and-error method. In this method, two ITO samples were etched using a specific recipe; after etching, the removal of the ITO was verified by measuring the current flow. The thickness of the ITO film determines the sheet resistance and hence the current flowing through it [33]. The solution used for Etching the ITO was a mixture of Hydrochloric acid and water. The ratio of HCL to water was 2:3. Hence for a 50ml solution, 30ml of water was mixed with 20ml of HCL solution. The HCL solution used was J.T. baker's 36.5% to 38% Hydrochloric acid. A total of two samples were used for this experiment, sample #1 was etched for 3 minutes, and sample #2 was etched for 5 minutes. The sample was strategically etched from the middle leaving the sides intact. Figure 16 and 17 shows the sample used for this experiment and the circuit used to measure the current.

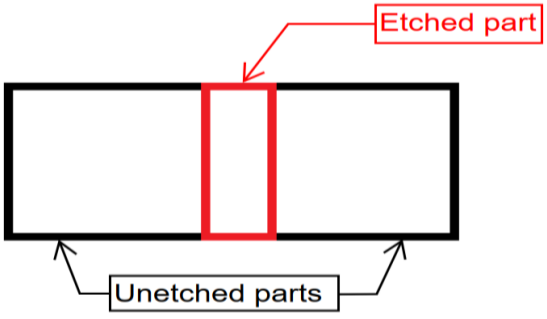

Figure 16: Sample used for determining the etch rate.

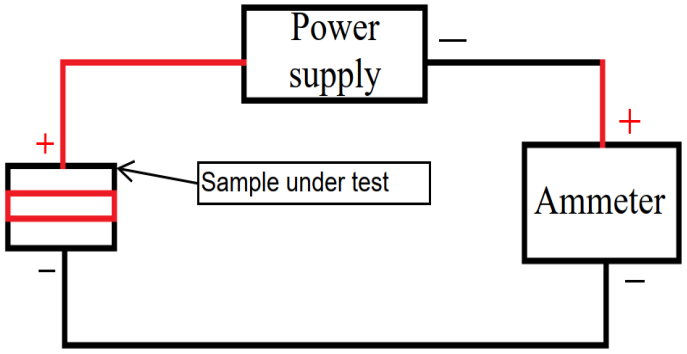

Figure 17: Current measurement circuit setup.

Using the setup shown in figure 17, current flow and hence the sheet resistance were determined. The table below shows the values obtained during the experiment.

Table 8: Results from the etching test done on ITO sample.

Parameters	Unetched ITO	Sample 1 (3 mins)	Sample 2 (5 mins)
Dimensions of the etched portion	-	2.5 cm x 0.4 cm	2.5 cm x 0.4 cm
Supply voltage	32 V	32 V	32 V
Measured current	9 mA	27 µA	0.0029 µA
Resistance	3.5 KΩ	1.18 MΩ	11 G Ω

After this examination, it was concluded that etching the patterned samples for 3 minutes results in the best dimensions of the electrode while maintaining the required isolation between the electrodes.

Once the recipe was known, the next step was to start etching the patterned ITO samples. Before putting the samples into the solution, the solution was heated up to 50°C to 55°C. After the solution reached the desired temperature, the patterned ITO samples were put into the solution for 3 minutes. After 3 minutes, the samples were removed from the solution and rinsed thoroughly; after rinsing, the samples were dried using nitrogen. After etching, it was necessary to make sure

that the top and the bottom sides of the electrode are separated. Hence a test was performed on the etched sample.

For ensuring the isolation of the top and the bottom part, it was necessary to make sure that no current is flowing from the top part to the bottom part. Hence, a current measurement test is performed on the sample. The figure below shows the setup used.

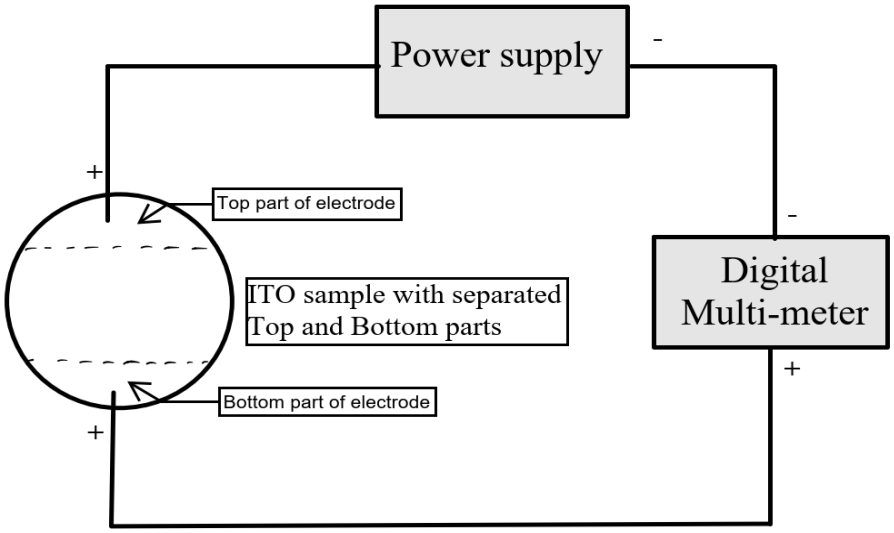

Figure 18: Circuit diagram for the current measurement setup.

Since the sample still has photoresist on the other parts except for the exposed portions, it needs to be removed before doing the above test. A small patch was created in the top, and the bottom of the sample for making the required contacts, as specified in the above setup. A brush dipped in the acetone was used to create the patch on the top and the bottom side of the ITO sample. After that, the sample was connected to the circuit in figure 18. If there is zero current flowing through the multimeter, then the top and the bottom parts are isolated.

7.5.2 Results

After this, the sample was again visually inspected under a microscope; below are the images of the etched sample under the microscope. The sample was inspected both before and

after, the photoresist was stripped off. Figure 19 shows the image of the etched sample after the resist is stripped off. The minimum measured spacing between the two electrodes is 145µm. However, the maximum spacing was 176µm.

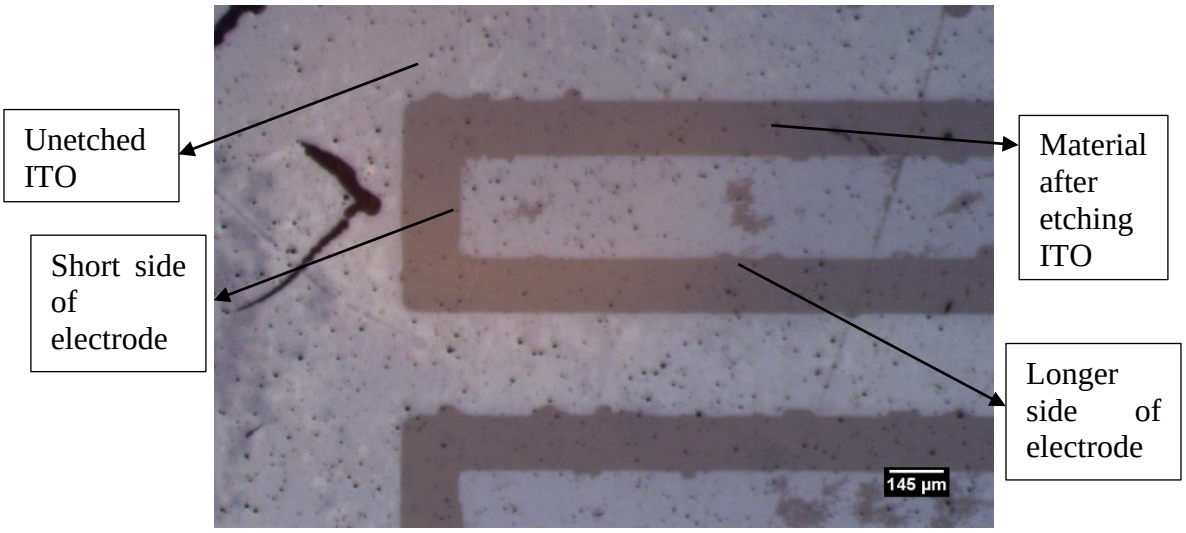

Figure 19: An image of the patterned and etched electrode on the ITO sample.

Figure 19 shows the top view of the electrode; for seeing how the electric fields are distributed between the electrodes, a cross-sectional view is needed to be considered. The figure below shows the cross-sectional view of the two electrodes after etching.

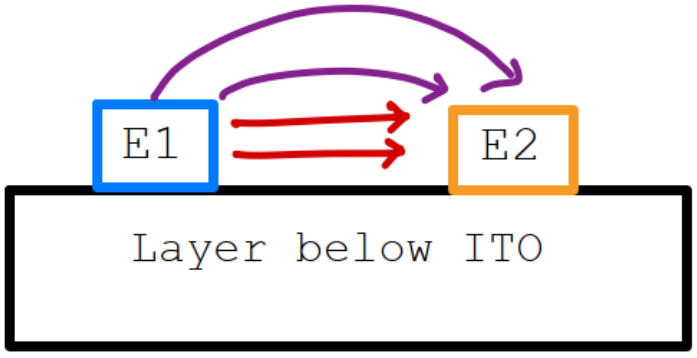

Figure 20: Cross-sectional view of one set of electrodes.

The above figure shows the expected field distribution between the two electrodes. In the above figure, the blue rectangle represents one electrode set, and the orange rectangle represents another (opposite) set of electrodes. The red arrows show the expected electric field that is expected to be generated between the two electrodes when the appropriate potential is applied. However, there is a high possibility that the fringing field (represented by purple lines) may be present. These fringing field lines rise above the electrode's structure, thereby increasing the effective area of intersection between the electrodes. A COMSOL simulation was performed for estimating the field distribution across the two electrodes. The figure below shows a similar structure used for simulation. The dimensions for the below structure is listed in table 9

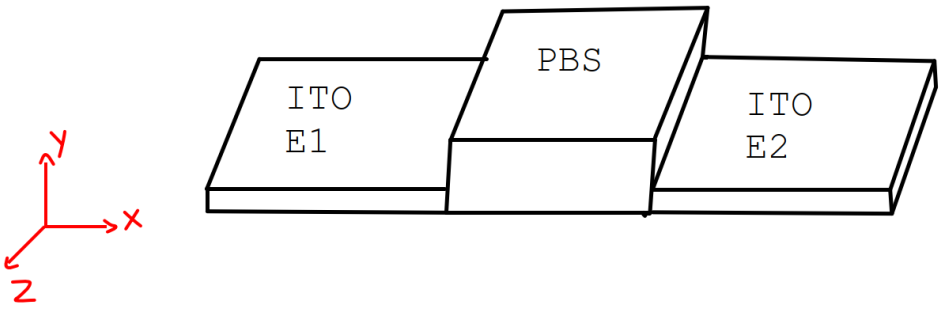

Figure 21: Cross-sectional diagram of the structure used in the simulation.

Table 9: Simulation parameters in COMSOL.

Parameters		Values
Physical dimensions	E1 and E2 (width)	3µm
	PBS width	135µm
	The thickness of E1 and E2	50nm
	Thickness of PBS	10µm
Electrical properties	Resistivity of ITO	1 x 10^{-4} Ω-cm
	The relative permittivity of ITO	1
	Conductivity of PBS	1 S/m
	The relative permittivity of PBS	80

Using the above parameters and the structure shown in figure 21 the following results were obtained.

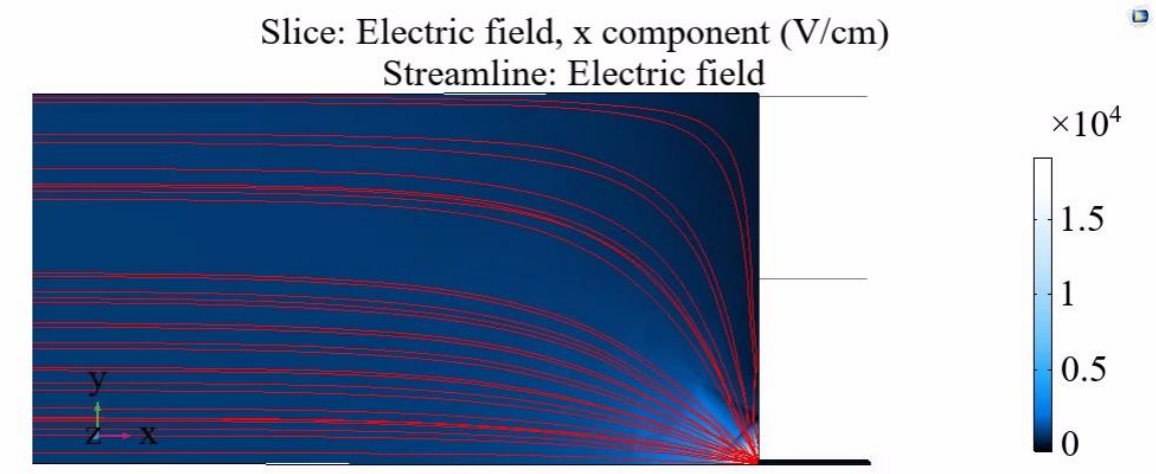

Figure 22: Simulated E-field distribution.

The figure above is the close-up view of the PBS and electrode intersection, the thin part on the bottom-right represents the ITO electrode, whereas the big blue block represents the PBS layer. The color chart represents the value of the x-component of the electric field across the PBS layer. The red lines in the above figure show the electric field lines between the two electrodes. Now if a vertical plate is kept at a distance of 0.5µm away from the E1 electrode the following is the electric field with respect to distance normal to the surface of the electrode.

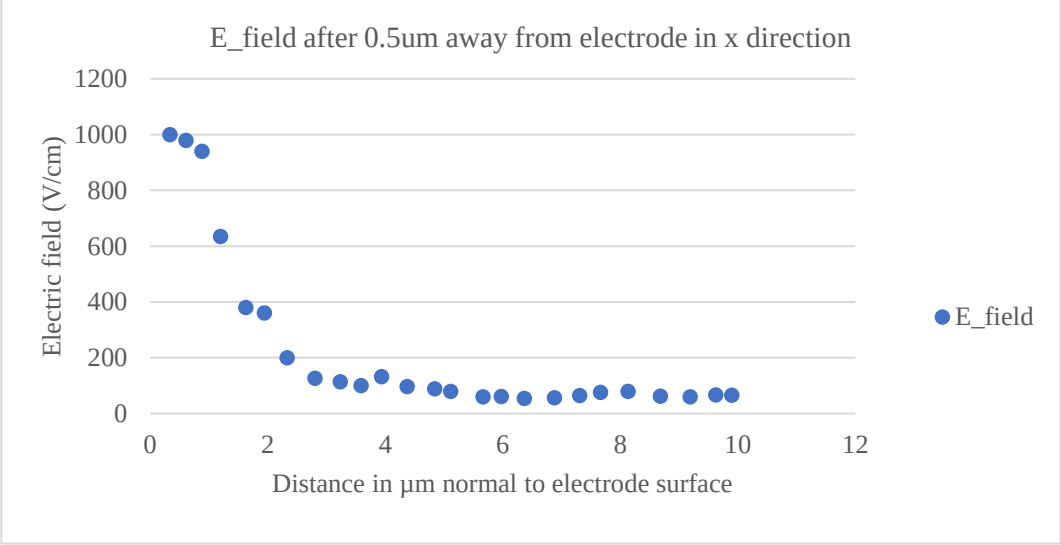

Figure 23: Estimated strength of E-field in y direction.

The reason for this graph in figure 23 is to estimate the strength of the fringing fields at a distance of 0.5 μm. The value on the x-axis represents the distance from the electrode in the direction normal to the electrode. And the values on the y-axis represent the strength of the electric field with respect to the x-axis values.

7.6 Silver Contacts on ITO

Once the sample is etched and the resist is stripped off the sample, the next step is to make ohmic contacts on the top and bottom electrodes. Making low resistance contact is to avoid significant voltage drop across the junction. These contacts were made using uninsulated copper wires. MG chemical's 8331 S silver epoxy was used for bonding copper wires with the ITO sample. Before the silver epoxy can be used, a test was conducted to inspect the conductivity of the silver epoxy on a few ITO samples. The accompanying sub-segment discusses applying silver epoxy to ITO samples; a similar methodology was used for the main ITO sample.

7.6.1 Procedure

Before using the silver epoxy to make copper contacts with the electrode, it is necessary to test the procedure for application. It is also essential to quantify the effect of using silver epoxy. Eighteen rectangular samples were used in this test; out of 18 samples, silver epoxy was applied on nine pieces, and no epoxy was applied to the other nine pieces. Note that the silver epoxy was only applied on one side of the strip. Figure 24 shows the image of a sample with silver epoxy (right sample) and without silver epoxy (left sample).

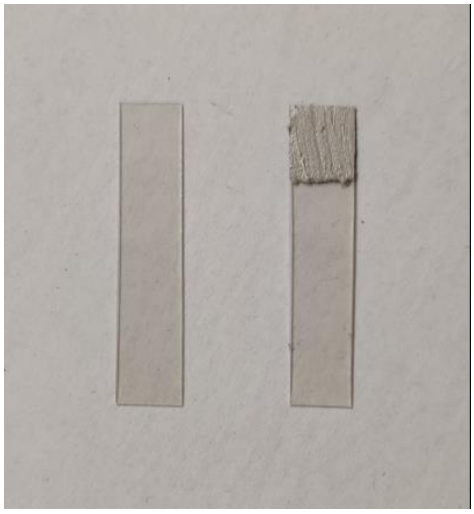

Figure 24: Sample used in the characterization of silver epoxy.

The following steps were performed for mixing and application of silver epoxy to the ITO sample.

1. Arrange the copper wire on the top of the ITO sample, as shown in the figure below. (A wooden board covered in aluminum foil can be used to keep under the sample for support).

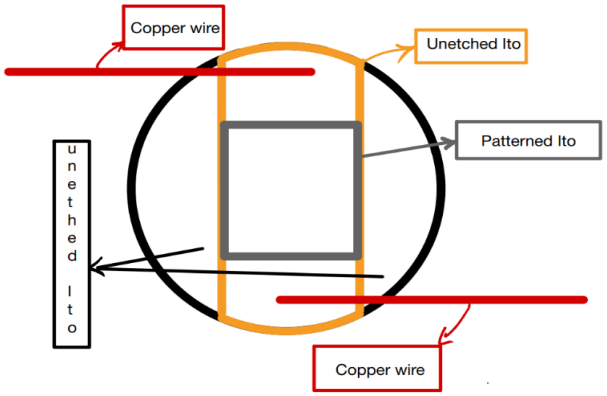

Figure 25: Arrangement of copper wires on the ITO sample.

2. Dispense equal amounts of both parts into a mixing tray.

3. Mix them for 2 minutes using a wooden stick or stirrer.

4. After done mixing, apply some epoxy to the copper wire and ITO intersection.

5. Heat the sample at 60℃ for 60 minutes.

While doing the characterization of the silver epoxy, step 1 was skipped. Table 10 in the results subsection shows the increase in the measured current due to the application of silver epoxy. The test setup for characterization was like the setup shown in figure 18. The above procedure was used to bond the copper wire with the electrode to make a low resistance contact in the electrode after applying the silver epoxy.

7.6.2 Results

This subsection talks about the results obtained from characterizing the silver epoxy on ITO.

Table 10: Test results from characterizing silver epoxy on ITO.

Sample #	Samples without Silver epoxy on them		Samples with silver epoxy on them	
	Applied voltage (V).	Measured current (mA).	Applied voltage (V).	Measured current (mA).
1	5	1.7	5	2.2
2		2.1		2.2
3		2.0		2.3
4		2.3		2.5
5		2.1		2.1
6		2.1		2.5
7		2.2		2.6
8		2.1		2.1
9		2.2		2.4
Average		2.088		2.322

The table above shows the current measurements taken from the eighteen samples under test. Also, figure 26 shows the graph obtained from the data in the table below

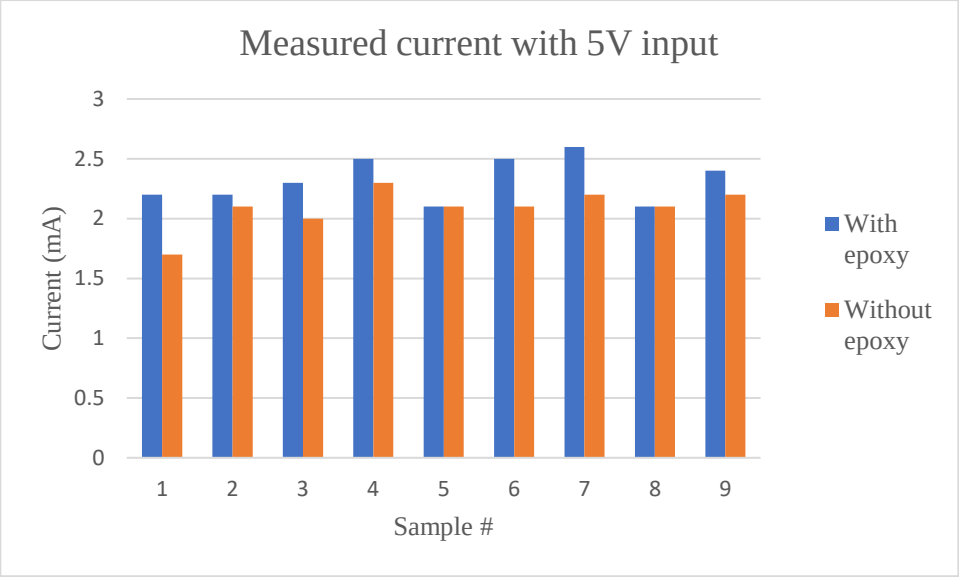

Figure 26: Graph of measured current during the characterization of silver epoxy.

In the above graph, the blue bar represents the current values for samples with silver epoxy on them, and the orange bar represents current values for samples without silver epoxy. As calculated in the table above, the average current increases by 30% when silver epoxy is applied.

7.7 Passivation

The intended use of this microelectrode array is to pulse cells that are suspended in PBS. PBS is a water-based salt solution. When potential is applied, copper and silver react with the PBS, resulting in the oxidation of copper and silver. Hence, to prevent this oxidation, a passivation layer is required. This passivation layer needs to be water and alcohol resistant since the electrode is intended to be washed and cleaned frequently. Gorilla 2-part epoxy was used to make this passivation layer; the procedure for mixing and applying the epoxy is shown in the following subsection.

7.7.1 Procedure

1. Dispense an equal amount of both parts of epoxy into a mixing cup.
2. Mix the epoxy for 2 minutes using an ice cream stick.
3. Apply the mixed epoxy on the copper wire as well as on the silver contact.
4. After the application, the epoxy sets in 5 minutes, but for complete cure, the epoxy must be cured for 24 hours; once the curing time is done, check for any exposed, uncovered parts. (During the application, care needs to be taken that the epoxy does not affect the electrode in any way. Also, the epoxy must be applied only in the lower parts of the copper wire.)

For checking that the epoxy is providing passivation, a continuity test can be performed using a multimeter. In the continuity test, one terminal of the multimeter was on the bare copper wire while the other terminal was on the passivated part of the copper wire. If the multimeter makes a beeping sound, it means that the passivation is not achieved. Figure 28 in the below subsection shows the electrode after contact passivation.

Before pulsing, it was necessary to know how many cells are sitting on the electrode and between the electrodes. This determines the ratio of treated cells to untreated cells. The cells that are between the electrodes experience an electric field and can be assumed as treated cells. However, the cells sitting on the electrode experiences nothing and hence can be assumed as untreated cells. Thus, to count the number of cells above and between the electrodes, the electrode with cells was examined under the microscope. Due to the transparent property of the ITO, the microscope was unable to differentiate between the electrode and spaces between the electrodes.

To overcome this problem, a sample was created using the same process as above but with a minor difference. The only difference was that the photoresist was not stripped off the ITO sheet after the etching was done. Hence now, the electrode has a coating of photoresist on its top. Due to the photoresist coating on the top of the electrode, the microscope detected the difference

between the electrode and spaces. The figure below shows the image taken from the eyepiece of the microscope.

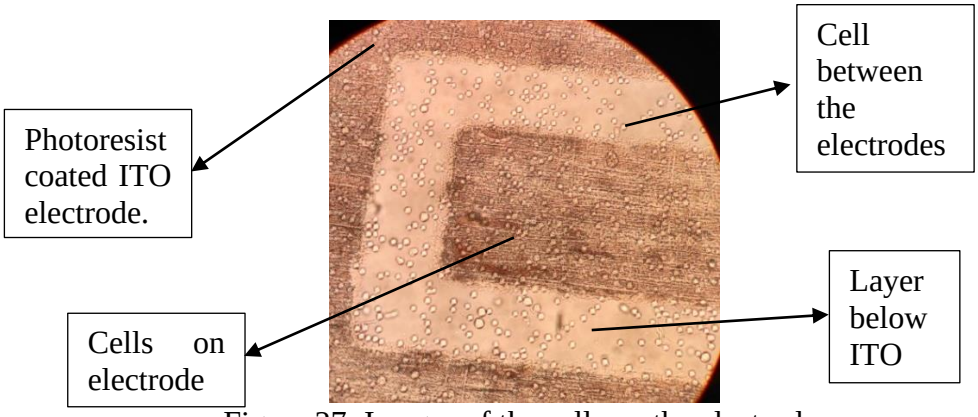

Figure 27: Images of the cells on the electrode.

The concentration of the cells here was 1 million cells per ml. increasing the concentration increases the number of cells between the electrodes. As seen in the figure, the width of the electrode is more compared to the spacing between the electrodes.

7.7.2 Results

The figure below shows the electrode after the application of the gorilla epoxy. As can be seen in the figure, a well-like structure is formed using epoxy. This is the area where the cells are expected to be. The reason for this kind of structure is to reduce the ratio of treated cells to untreated cells. If the epoxy is only applied near the contact area, then the electrode can accommodate more volume of cells. However, the only area where the cells are treated is in the center, where the interdigitated pattern is. This reduces the ratio of treated to untreated cells. Also, the cells in the areas other than the electrode are of no use. Hence to increase the proportion of treated to untreated cells and reduce the use of Sytox, a well-like structure was formed using the

epoxy. This design not only reduces the amount of Sytox required for each trial but also increases the chances of selecting treated cells.

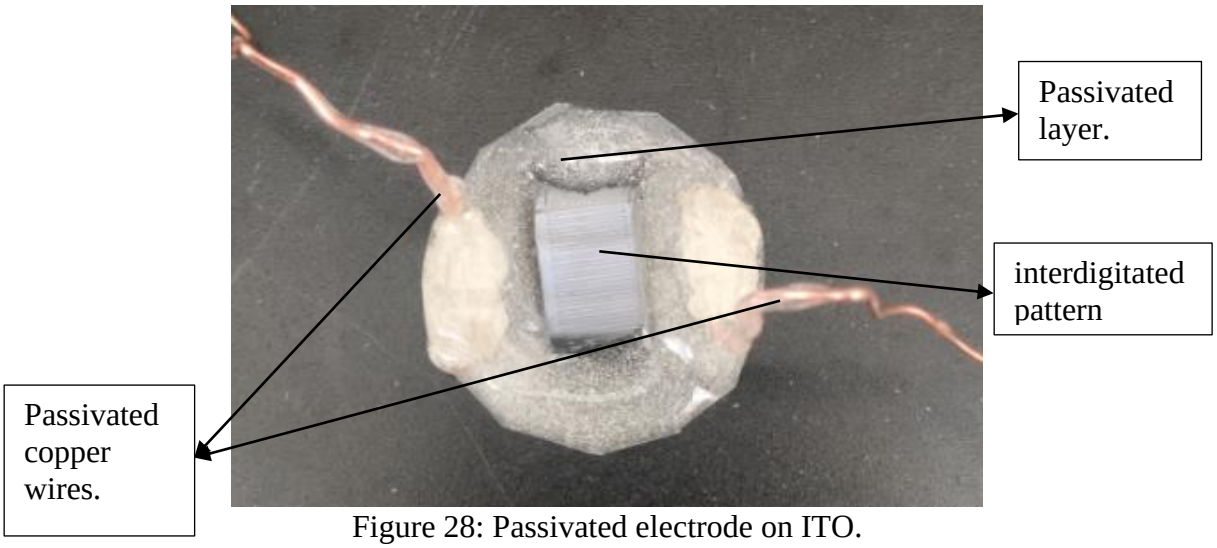

Figure 28: Passivated electrode on ITO.

7.8 Pulsing with PBS

Once the electrode is ready, it is time to test the electrode. For testing the electrode, two pulsing circuits were used. The figure below shows the initial pulsing circuit used, and figure 31 shows the modified pulsing circuit.

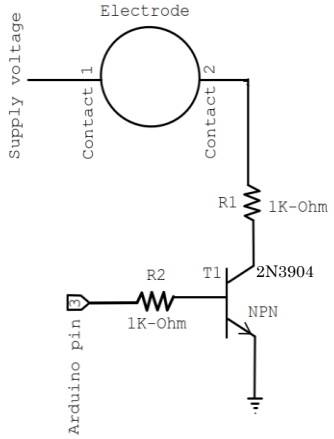

Figure 29: Initial pulsing circuit.

The pulsing circuit above was used initially to pulse the PBS, and the graph in figure 30 is obtained when PBS was pulsed using the above circuit. The pulse in the figure below is the voltage measured at C2 contact of the electrode (in figure 28) with reference to ground.

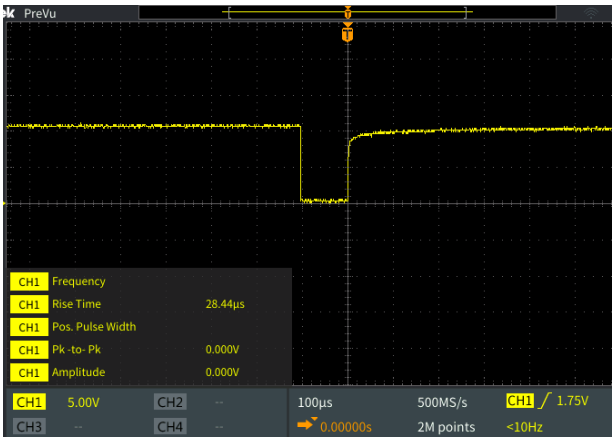

Figure 30: Pulse obtained from the initial circuit.

As seen in the figure above, the electrode's contact 1was continuously at supply voltage. Once the T1 is turned on, it connects contact 2 to the ground for 100µsec, resulting in the pulse shown in the figure above. As seen in the graph, the voltage at C2 is always at the supply voltage, and it is pulled down to 0 volts when T1 is turned on. Another approach to achieve a pulse can be to keep the voltage at the C2 terminal of the electrode equal to zero and only raise it to the supply voltage for 100 µsec. Hence creating a pulse. The circuit in figure 31 is used for this approach, and this circuit results in a pulse shown in figure 33.

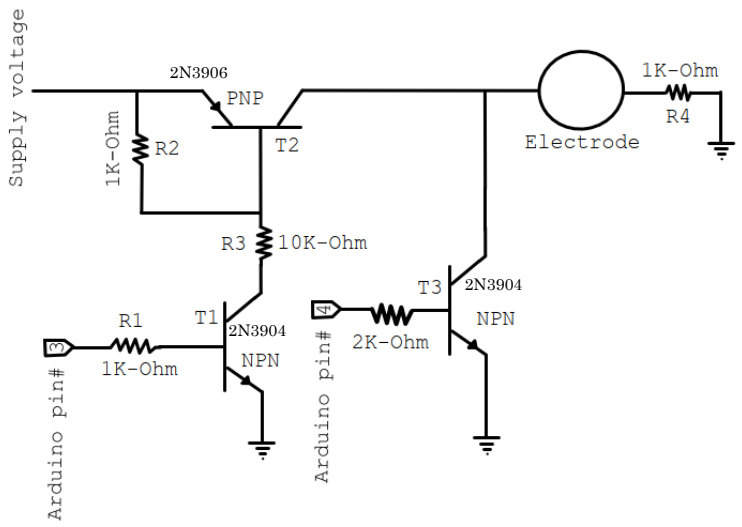

Figure 31: Final pulsing circuit.

The following sub-section talks about the procedure used for pulsing. The procedure is designed in such a way that it created a square pulse of approximately 100µsec to 110µsec.

7.8.1 Procedure

The below algorithm was used to produce the square waveform from the circuit in figure 32.

1. Turn on the transistor T1.
2. Wait for 80µsec. Then turn T1 OFF.
3. Wait for 20µsec and then turn T3 ON.
4. Wait for 10µsec and then turn T3 OFF.
5. Wait for 500msec, repeat the process.

The above procedure was converted into the Arduino code, figure 32 shows the screenshot of the Arduino code used. Table 11 shows the pulse parameters that were used for pulsing the PBS

on the electrode. The supply voltage was set to 14 Volts during the pulsing. These parameters were obtained from the graph shown in figure 33.

```
const int transistor = 3;
const int t2 =4;

void setup()
{
  pinMode (transistor, OUTPUT);
  pinMode (t2, OUTPUT);
   }


void loop()
{
   digitalWrite (transistor, HIGH);
  delayMicroseconds(80);
  digitalWrite (transistor, LOW);
  delayMicroseconds(20);
  digitalWrite(t2, HIGH);
  delayMicroseconds(100);
  digitalWrite(t2,LOW);
  delay(500);
}
```

Figure 32: Arduino code used for pulsing cells.

Table 11: Pulse parameters.

Serial number	Parameter	Value
1	Supply Voltage	14 V
2	Pulse width	105µ sec
3	Time between 2 pulses	500m sec
4	Pulse amplitude	15.75 V
5	Fall time	46.05n sec
6	Frequency	2 Hz

For pulsing, 700µL of PBS was put on the electrode before pulsing. The voltage across the electrode and the current through the electrode were measured. For measuring the current through the electrode, a 1kΩ resistor was connected in series with the electrode. The value of the resistor was determined such that no more than 5% (with a tolerance of 1%) of the supply voltage is dropped across the resistor. The reason for the tolerance is because of the limitations of fixed resistor values.

7.8.2 Results

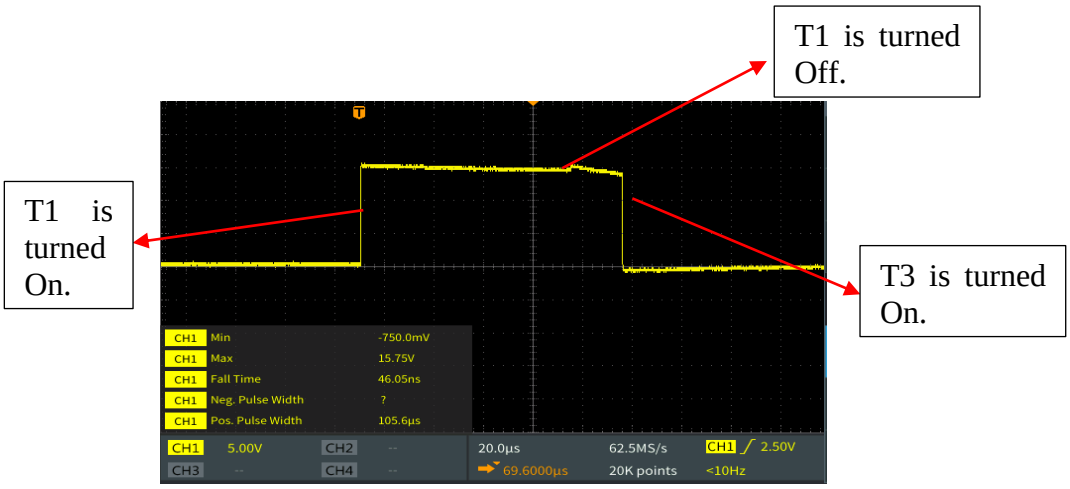

Figure 33: Graph showing the characteristics of the pulse used in the experiment.

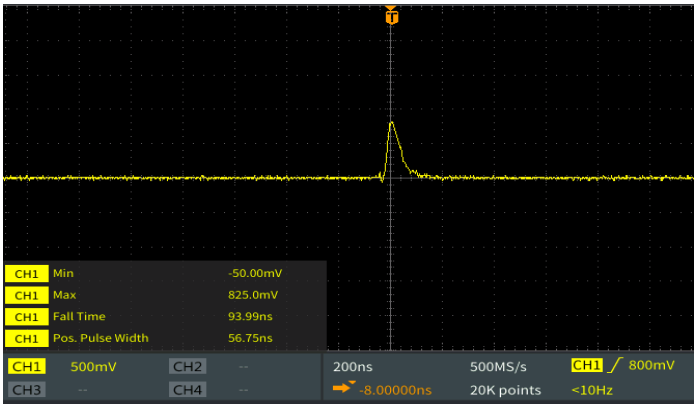

Figure 34: Graph of the voltage drop across resistor R4 used in figure 31.

7.8.3 Conclusion

The graph in figure 34 shows the voltage drop across the resistor; note that the voltage drop only occurs when there is a change in the supply voltage, i.e. when switching from low to high voltages and vice versa; this means that the current through the electrode is only flowing when there is a change in the supply voltage. Hence it implies that the electrode is capacitive, i.e., it behaves like a capacitor. The load acts like an RC circuit; it takes some time to discharge when the power is removed; to avoid this delay, another NPN transistor T3 was connected; this transistor was turned on 20µsec after the transistor T1 was turned off. The reason to wait before T3 can be

turned on is to make sure the current is only flowing through the electrode. Also, it is noteworthy that the voltage drop across the resistor is 825mV below 6% of 14 Volts. This voltage drop can be used to calculate the amount of current flowing through the electrode. Since the current in series is equal, the current flowing through the resistor is equal to the current flowing through the electrode. Applying Ohm's law to calculate the current through a 1k-ohm resistor with 825mV of a voltage drop across it results in 825µA of current flowing through the resistor. Hence the amount of current flowing through the electrode is equal to 825µA. The time for which the current flows is approximately 56nsec, as seen in the graph from figure 34. Considering that the current is flowing uniformly between all the arms of the electrode, an approximate 58nA of current is flowing per micrometer length. For pulsing, 20 such pulses were passed from the power supply to the electrode. The same 20 pulses with the same characteristics were used to pulse the cells on the electrode.

7.9 Electroporation of Cells

Finally, once the electrode and the pulsing circuit are ready, it is time to start experimenting on the cells. The procedure used to experiment on cells is mentioned in the following sub-section.

7.9.1 Procedure

Before the experimentation, cells were cultured into a canted neck flask to an optimum concentration. No experiments were performed when the cell concentration was more than 3 million per ml. If the cells are within the optimum concentration range, then the cells are washed twice with PBS. For washing the cells, Eppendorf's centrifuge was used. The cells were spun at 150rpm for 3 minutes. After washing, they are suspended in PBS such that their concentration is

between 1 to 1.5 million per ml. The amount of PBS added in the cells to obtain desired concentration was calculated using the formula below.

$$initial\ concentration * initail\ volume = final\ concentration * final\ volume$$

Once the cells are at the desired concentration, the pulsing circuit was set in the same configuration as shown in figure 31. Sytox^{TM} green was obtained from the manufacturer as a 5mM solution in DMSO. It was diluted to a 5µM solution in PBS. The concentration was obtained from document 34 in the reference section [34]. The following formula was used to calculate the amount of Sytox required.

$$amount\ of\ sytox * 5\mu M = (volume\ of\ cell\ suspension + amount\ of\ sytox) * 1\mu M$$

After pulsing, 175µL of 5µM Sytox^{TM} was added to the pulsed cells to get a concentration of 1µM, and the solution was mixed by gentle pumping using a pipet. The following procedure was followed for conducting one trial.

1. Connect the electrode to the pulsing circuit, as shown in figure 31. The resistor was selected such that the voltage drop across it is approximately less than 5% of the total load voltage value.

2. Put 700µL of cells suspended in PBS on the electrode for one trial and on the other well-plate as control. The cells were only on the electrode and were not touching walls of the well plate or copper wires connected to the electrode.

3. Wait for 10 minutes and let the cells settle. While waiting for cells to settle, it was made sure that the electrode and the well plate is steady and not moving. If the well plate moves, 10 minutes of additional wait time was added.

4. After 10 minutes, set the appropriate voltage on the power supply. Since in this electrode, electroporation is achieved using an electric field, the voltage needs to be calculated depending upon the distance between the two electrode fingers. The following formula was used to calculate the supply voltage for a given electric field.

$$Electric\ Field = \frac{Voltage}{Distance}$$

Now with electrodes with a separation of 145µm. And a supply voltage of 14 V, a 965.72 V/cm of the electric field, is generated.

5. Turn ON the power supply and wait for 10 seconds, then turn OFF the power supply. The pulsing scheme used for the experiment was the same as the one used for pulsing PBS, and the pulse parameters are shown in table 11 of section 7.8.1.

6. Immediately put 175µL of 5µM Sytox™ into the cell solution. Then gentle pump with a pipet. While adding the Sytox™, it was made sure that the pipet is touching the ITO. The Sytox™ was added to the treated cells no more than 2 minutes after the pulsing was stopped. The solution was mixed by gently pumping the solution using the pipette. The solution was pumped five times for mixing. After adding the Sytox™ to the treated cells, Sytox™ was added to the control cells as well. Again, for mixing, the solution was gently pumped five times using the pipette.

7. Put 150µL of control cells and treated cells into the plate reader plate in the fashion shown in the figure below.

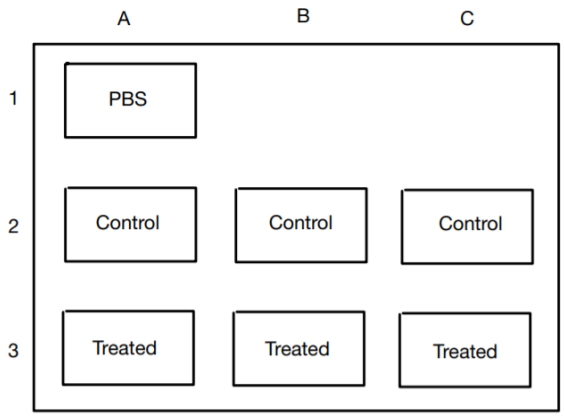

Figure 35: Sample allotment of cells into the plate reader.

Total three samples from each control and treated solution were put into the 96 well culture plate. Before placing the plate into the plate reader, BioTek's Gen5 Data Collection and Analysis Software was opened in the computer connected to the plate reader. From the list of protocols, the *"sytoxKinetic_10_minutes.prt"* protocol was selected.

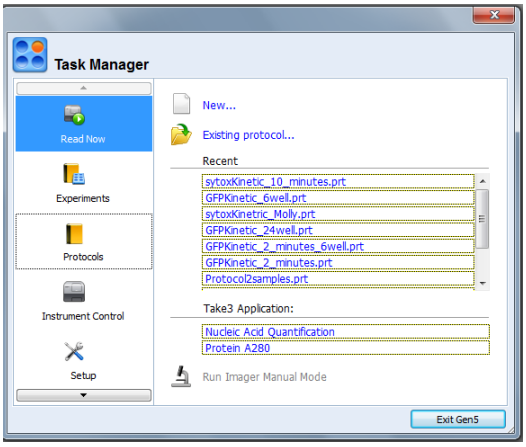

Figure 36: A screenshot of the list of available protocols.

After that, the wells are selected to read. The following figure shows the software screen during the selection of well plates to read.

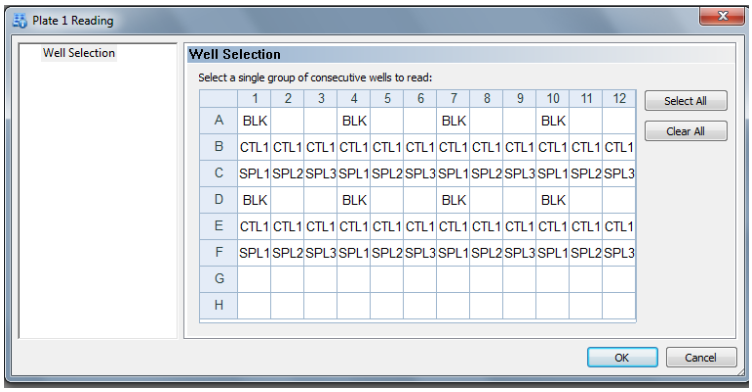

	1	2	3	4	5	6	7	8	9	10	11	12
A	BLK			BLK			BLK			BLK		
B	CTL1	CTL1	CTL1	CTL1	CTL1	CTL1	CTL1	CTL1	CTL1	CTL1	CTL1	CTL1
C	SPL1	SPL2	SPL3	SPL1	SPL2	SPL3	SPL1	SPL2	SPL3	SPL1	SPL2	SPL3
D	BLK			BLK			BLK			BLK		
E	CTL1	CTL1	CTL1	CTL1	CTL1	CTL1	CTL1	CTL1	CTL1	CTL1	CTL1	CTL1
F	SPL1	SPL2	SPL3	SPL1	SPL2	SPL3	SPL1	SPL2	SPL3	SPL1	SPL2	SPL3
G												
H												

Figure 37: Figure showing the screen for selecting plates to read.

Note here that only the wells containing the cell solution and the well with PBS are selected, and this selection changes with each trial. After choosing the plates, hit okay. After hitting okay, the plate reader starts warming up.

8. Once the plate reader is ready, put the plate into the plate reader. Once the plate is inside the plate reader, press enter on the computer, and the plate reader will start reading. To see the fluorescence data, select the appropriate well plates. The fluorescence data of the cells is shown in the 7.9.2 section. A total of 3 experiments with a minimum of 3 trials were performed [20, 21, 34].

9. Check the viability of the treated and control cells. After putting the cells into the plate reader, check the viability of the cells by doing the trypan blue exclusion test. This is the same test that was done while accessing the biocompatibility of the ITO. Checking the viability of cells after electroporation is necessary to validate the fluorescence data. As established before, Sytox^{TM} glows when it comes in contact with the nucleic acid. Hence, we can get fluorescence data even if the cells are dead. The high viability of cells after the procedure eliminates that

possibility. However, the viability was only measured for the cases where the fluorescence of the treated cells is higher than the control cells.

10. Clean the electrode and the culture plate with alcohol. Once the trial is done, remove the extra cells into a container and then clean the electrode and culture plate with alcohol. The electrode was cleaned with a cotton swab; the alcohol was sprayed on the cotton swab before cleaning the electrode.

7.9.2 Results

Figure 38 shows the typical result obtained after performing one trial. The y axis is the arbitrary fluorescence units, and the x-axis is time. The graph in figure 38 represents the data obtained from the second trial of the first experiment.

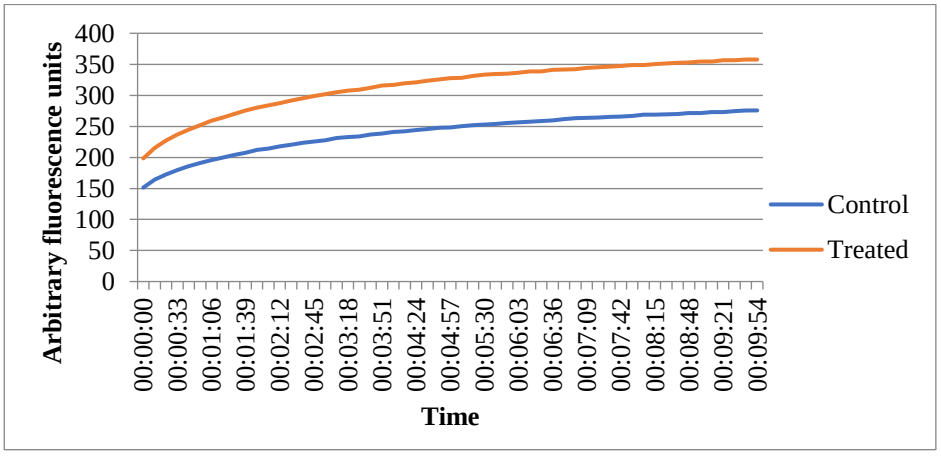

Figure 38: Example of obtained fluorescence data.

The final data point value (value at 00:09:54) was selected. Table 12 shows the florescence values obtained from the experiments. As seen in the table minimum of three trials were conducted per experiment. The C1, C2, and C3 values in table 12 represent the fluorescence data for control cells. Similarly, T1, T2, and T3 values represent the fluorescence data for the treated cells. The

average fluorescence for control was calculated by averaging the C1, C2, C3 values, and the average fluorescence for treated cells was calculated by averaging the T1, T2, T3 values.

Table 12: Experiment results.

Experiment #.	Trial no.	Time in hours	C 1	C 2	C 3	T 1	T 2	T 3	Average control for each trial	Average treated for each trial
1	1	0.5	309	279	243	327	308	266	277	300.33
	2	1	243	286	298	328	347	398	275.67	357.67
	3	1.5	220	299	305	363	278	288	274.67	309.67
	4	2	283	288	289	278	294	289	286.67	287
	5	2.5	359	373	349	341	338	359	360.33	346
2	1	0.5	366	390	318	394	370	395	358	386.33
	2	1	258	274	287	331	327	364	273	340.667
	3	1.5	506	498	457	556	554	582	487	564
	4	2	494	510	543	563	513	486	515.67	520.67
3	2	1	291	354	292	374	405	332	312.33	370.33
	3	1.5	354	351	332	414	395	334	345.67	381
	4	2	321	337	341	323	323	327	333	324.33
	5	2.5	327	336	320	285	266	282	327.67	277.67
4	1	0.5	381	383	334	385	385	430	366	400
	2	1	430	431	414	424	445	450	425	439.67
	3	1.5	419	401	385	478	457	442	401.67	459
	4	2	487	464	476	445	457	448	475.67	450
5	1	0.5	391	371	331	435	357	637	364.33	476.333
	2	1	414	402	415	398	362	364	410.33	374. 67
	3	1.5	401	457	378	491	482	409	412	460.67
6	1	0.5	430	446	361	505	546	525	412.33	525.33
	3	1.5	522	495	554	570	509	578	523.67	552.33
	5	2.5	629	506	554	537	517	622	563	558.67

In table 12, the time column represents the time elapsed (in hours) after the cells are separated from the culturing media and suspended into PBS. It is necessary to keep track of time because there is a direct relationship between the time elapsed and the measured arbitrary fluorescence values. The arbitrary fluorescence increases with the amount of time for which the

cells are suspended in PBS [35]. From table 12, all experiments start after 30 mins from the time cells are removed from the culture media. In these 30 minutes, the cells are washed and diluted to the desired concentration with PBS.

Table 13: Average fluorescence for control and treated cells for each experiment.

Expt #.	Average control for each trial	Average treated for each trial	Average control for each experiment	Average treated for each experiment	SD for control of each experiment	SD for treated of each experiment
1	277	300.33	294.867	320.133	33.012	27.119
	275.67	357.67				
	274.67	309.67				
	286.67	287				
	360.33	346				
2	358	386.33	408.416	452.916	98.1080	92.145
	273	340.667				
	487	564				
	515.67	520.67				
3	312.33	370.33	329.667	338.333	11.95	40.99
	345.67	381				
	333	324.33				
	327.67	277.67				
4	366	400	417.083	437.167	39.817	22.522
	425	439.67				
	401.67	459				
	475.67	450				
5	364.33	476.333	395.556	437.222	22.087	44.6934
	410.33	374. 67				
	412	460.67				
6	412.33	525.33	499.667	545.444	63.807	14.453
	523.67	552.33				
	563	558.67				

Table 13 shows the average fluorescence for each experiment. The average fluorescence for one experiment was calculated by taking the average of the fluorescence values for all trials in that experiment. The mean for each experiment is calculated to analyze if the fluorescence is

changing with each experiment. Along with the average of the fluorescence data, a standard deviation of the data is also calculated in table 13. The significance of calculating standard deviation is to figure out the data spread, i.e., how far are the data points from the mean.

The graph in figure 39 shows the plot of average fluorescence for control and treated cells for each experiment. As seen in the figure, the standard deviation of both the control and the treated cells overlaps. An overlapping standard deviation is not an expected parameter here. An overlapping standard deviation implies that the data is not statistically significant. More the overlapping less the probability of the data to be statistically significant.

Figure 39: Plot for average fluorescence values and standard deviation.

The reason for this large standard deviation is the large spread of the data. A T-test is also performed to determine the statistical significance of the data. Table 14 below shows the T-test results for each experiment. These individual experiments can be combined since all these experiments were performed under the same conditions. Hence, they can be combined to analyze the overall significance of the data. In a T-test, for statistical significance, the value of T_{stat} should

be greater than the value of the $T_{critical}$. Also, the probability should be less than 0.05. This value of probability less than 0.05 signifies that less than 5 % of the data is random, but the other 95% is statistically significant. Hence from table 14, it can be concluded that even though the fluorescence of the treated cells is higher than the control cells, the data is not statistically significant.

Table 14: T-test data for experiments when all trials are considered.

Experiment no.	T_{stat}	$T_{critical}$	Probability of significance (1-tail)
1	1.18	1.85	0.13
2	0.57	1.94	0.29
3	0.35	2.13	0.37
4	0.76	2.01	0.24
5	1.18	2.35	0.16
6	0.98	2.91	0.21
Considering all experiments as one experiment	1.13	1.68	0.13

However, if the trials performed after a time span of 1.5 hours are not considered in each experiment, things get interesting. The reason for excluding the trials after 1.5 hours is that the fluorescence value of the treated cells is equal to the fluorescence value of control cells. Table 15 shows the experiments without considering trials after 1.5 hours, and table 16 shows the corresponding average values of fluorescence for the control and treated cells. As seen in Table 15, some of the experiments do not have a minimum of three trials per experiment. The reason for only two trials in 1.5 hours' time span is because of operational errors. The operational error was occurring on the plate reader results in invalid read values. This error occurs when the plate holder moves to its home position in too few or too many steps.

Table 15: Average fluorescence values from an experiment with selected trials.

Experiment #.	Trial no.	Time in hours	C 1	C 2	C 3	T 1	T 2	T 3	Average control for each trial	Average treated for each trial
1	1	0.5	309	279	243	327	308	266	277	300.33
	2	1	243	286	298	328	347	398	275.67	357.67
	3	1.5	220	299	305	363	278	288	274.67	309.67
2	1	0.5	366	390	318	394	370	395	358	386.33
	2	1	258	274	287	331	327	364	273	340.667
	3	1.5	506	498	457	556	554	582	487	564
3	2	1	291	354	292	374	405	332	312.33	370.33
	3	1.5	354	351	332	414	395	334	345.67	381
4	1	0.5	381	383	334	385	385	430	366	400
	2	1	430	431	414	424	445	450	425	439.67
	3	1.5	419	401	385	478	457	442	401.67	459
5	1	0.5	391	371	331	435	357	637	364.33	476.333
	2	1	414	402	415	398	362	364	410.33	374. 67
	3	1.5	401	457	378	491	482	409	412	460.67
6	1	0.5	430	446	361	505	546	525	412.33	525.33
	3	1.5	522	495	554	570	509	578	523.67	552.33

Table 16 shows the calculated average fluorescence values with their respective standard deviations for all experiments. From the standard deviation values, it can be predicted that there is still a chance of overlapping standard deviation for the control and treated cells. This claim can be seen in the graph in figure 40, which is plotted from the data in table 16. As seen in the graph from figure 40, the standard deviation of 3 experiments out of 6 experiments does not overlap. This suggests a better possibility for getting statistically significant data for this set of trials. However, the overlapping standard deviations for the remaining three experiments are high. Hence a T-test is required to be performed.

Table 16: Average fluorescence values and SD for selected trials.

Expt #.	Average control for each trial	Average treated for each trial	(%) Viability		Average control for each Expt	Average treated for each Expt	SD for control of each Expt	SD for treated of each Expt
			C	T				
1	277	300.33	-	-	275.778	322.556	0.9558	25.117
	275.67	357.67	77	98				
	274.67	309.67	89	99				
2	358	386.33	97	96	372.667	430.333	87.978	96.337
	273	340.667	95	95				
	487	564	98	95				
3	312.33	370.33	97	97	329	375.667	16.666	5.333
	345.67	381	92	97				
4	366	400	94	94	397.556	432.89	24.261	24.55
	425	439.67	91	92				
	401.67	459	94	93				
5	364.33	476.333	94	94	395.556	437.22	22.087	44.693
	410.33	374. 67	-	-				
	412	460.67	90	93				
6	412.33	525.33	89	97	468	538.83	55.666	13.5
	523.67	552.33	98	90				

Figure 40: Plot for average fluorescence values and standard deviation for selected trials.

The T-test was performed for each experiment and for the case where all the experiments are treated as one experiment. Again, grouping all the trials under one experiment is because all

the trials were performed under the same conditions. Table 17 shows the performed T-test on the new set of trials. In the table below the data suggests no statistical significance for any of the experiments, but when all the trials are combined under one experiment and treated as one data set, the resulting T-test suggests that the data obtained are statistically significant. Hence, overall, the data is statistically significant, but when each experiment is examined as one, none of the experiments are statistically significant even though the standard deviation of few experiments does not overlap.

Table 17: T-test analysis for selected trials per experiment.

Experiment no.	T_{stat}	$T_{critical}$	Probability of significance (1-tail)
1	2.63	2.91	0.05
2	0.62	2.13	0.28
3	2.66	6.31	0.11
4	1.44	2.13	0.11
5	1.18	2.35	0.16
6	1.23	6.31	0.21
Considering all experiments as one experiment	1.74	1.69	0.04

The reason for this low statistical significance is the lower values of fluorescence obtained from the treated. This could be due to multiple reasons; maybe the cells are not settling entirely in 10 mins of a given time, or perhaps the electrode is somehow not generating the required electric field everywhere on the electrode. For verifying the second claim, the electrode was again examined under the microscope after six experiments, and below are the image obtained.

As seen in figure 41, there are multiple broken electrode arms. Due to these fractured arms, the number of treated cells reduces, resulting in lower fluorescence values. This wear and tear of the electrode can be a result of cleaning it after each trial. Even though it is established that the electrode has few broken arms, it is not established that when this happened, and hence it is hard

to say if that is the only reason or one of the many reasons why the fluorescence value is not statistically larger than the control.

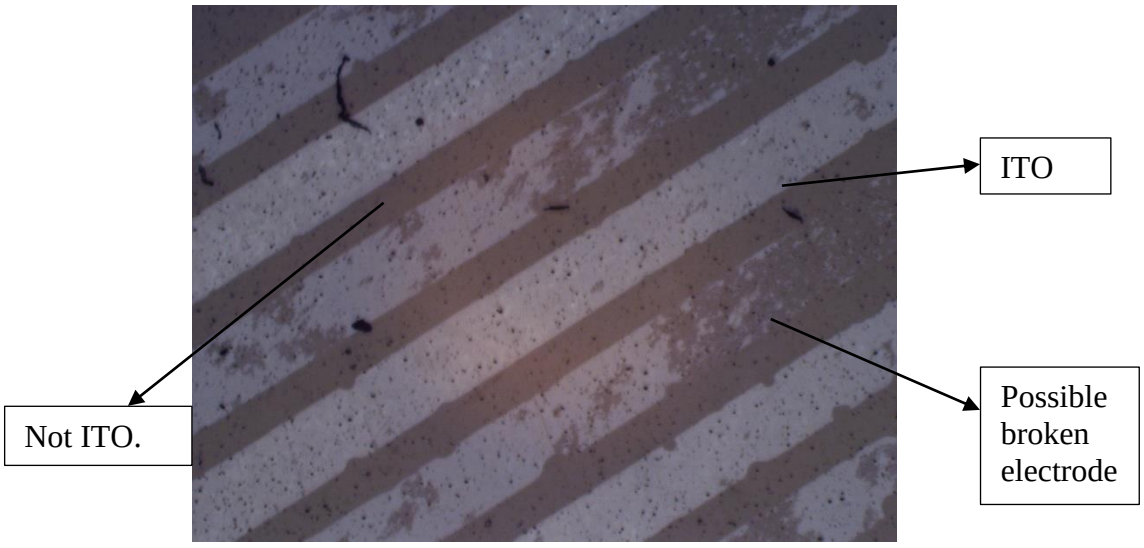

Figure 41: Electrode after performing six experiments.

Another reason for the lower fluorescence value could be that the ratio of treated cells to untreated cells is very low. The reason for this low ratio is the mask design parameters. The electrode array designed had an electrode thickness of 20pixels, and the spacing between the electrodes was 9 pixels. Hence if calculated, the electrode arm is twice as thick compared to the spacing between the arms. Therefore, the cells that are not treated are double in numbers compared to the treated cells considering that all the cells in between the electrodes are treated. Hence at best, only 50% of the cells on the electrode are treated. A newer electrode could be designed with a lower width of electrode arms. An electrode with similar specifications was intended as a part of this research, but it was not tested. The figure below shows the image of the electrode. Here the thickness of the electrode arms is reduced to 10 pixels while keeping the distance between the arms as 9 pixels.

As seen in figure 42, the electrode arms are now thinner than those in figure 41. However, it can be seen that there are few breaks and undercuts in the electrode, and coating ITO can avoid these cuts with HMDS before coating it with resist. Hence a trade-off needs to be done between the width of the electrode and the ratio of treated to untreated cells.

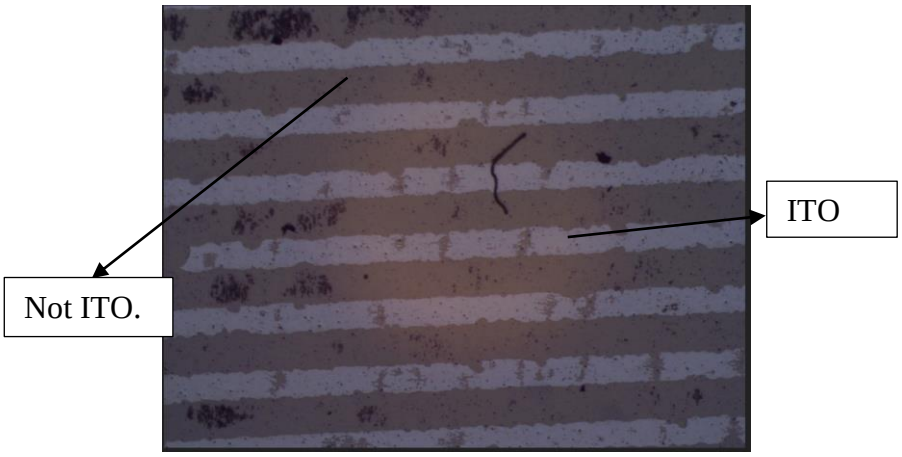

Figure 42: Modified electrode.

7.9.3 Conclusion

The goal of this research was to fabricate a planar microelectrode array that can produce high electric fields using low voltages. Achieving a high electric field using low voltage is possible by reducing the distance between the electrodes. Many devices were fabricated using the same principle, and this research contributes to that field of study. The advantage of this device is that it is transparent, which allows the user to see the cells on the electrode under a microscope. Being able to see the cell during the experiment is helpful, particularly to study the effects of the electric field on the cell.

According to the discussion in the above section, it is seen that the data is still premature, and it is too soon to draw any conclusions about the functioning of the device. However, the obtained data suggest that the device is conditionally functioning. The reason for this is that the

trials performed before 1.5 hours give fluorescence values higher than the control. However, the tests performed after 1.5 hours resulted in fluorescence values of control same as that of the treated cells. Hence, it can be said that the electrode stops working after 1.5 hours. Also, it is essential to note that the device functions appropriately for the next set of experiments, performed after a minimum of 2 days. Hence there are still many parameters and variables that are needed to be tested before drawing any conclusion. The possible future work for this device is stated in chapter 8.

Chapter 8: Future Work

For the previous sections, it can be concluded that the data obtained is premature to draw any conclusions; however, more experiments can be performed on the electrode to determine the causes for certain aspects of the system. One example will be to see the effect of time on the fluorescence data and how the time for which cells are out affects the fluorescence value. Another analysis could be to examine the number of experiments that can be performed on a single electrode. Further work can be done to make a better and efficient electrode.

As seen in the section above, a newer electrode design could be used where the ratio of treated cells to untreated cells is more. Figure 42 shows such an electrode where the width of the electrode arm is less than the initial electrode. Using the electrode in figure 42, the relationship between the electrode arm thickness and the fluorescence data can be investigated.

Another modification to the current electrode could be increasing the active region. Here the active area means the region in which the electrode is etched. As seen in figure 28, the electrode is only in the center part, and the rest of the ITO is etched away; the region in which the electrode is could be increased by using a bigger mask. Increasing the active area increases the volume of cells the electrode can hold. Few other improvements could be made in the fabrication process, especially in the passivation section. An epoxy mold can be used to create a perfect, well-like structure. Using a mold reduces the chances of epoxy falling on the electrode area rendering the whole sample useless. Finally, a better lithography process could be used to reduce the cuts in the electrode.

References

[1] G. A. R. Gonçalves and R. M. A. Paiva, "Gene therapy: advances, challenges and perspectives," *Einstein (Sao Paulo, Brazil)*, vol. 15, no. 3, pp. 369-375, Jul-Sep 2017, doi: 10.1590/s1679-45082017rb4024.

[2] E. H. Kaji and J. M. Leiden, "Gene and stem cell therapies," (in eng), *Jama*, vol. 285, no. 5, pp. 545-50, Feb 7 2001, doi: 10.1001/jama.285.5.545.

[3] H. T. Greely, "Ethical Issues in the 'New' Genetics," in *International Encyclopedia of the Social & Behavioral Sciences*, N. J. Smelser and P. B. Baltes Eds. Oxford: Pergamon, 2001, pp. 4762-4770.

[4] L. A. U. Jane B. Reece, Michael L. Cain, Steven A. Wasserman, Peter V. Minorsky, Robert B. Jackson, *Campbell Biology*. 2009.

[5] O. Bleiziffer, E. Eriksson, F. Yao, R. E. Horch, and U. Kneser, "Gene transfer strategies in tissue engineering," (in eng), *Journal of cellular and molecular medicine*, vol. 11, no. 2, pp. 206-23, Mar-Apr 2007, doi: 10.1111/j.1582-4934.2007.00027.x.

[6] S. Misra, "Human gene therapy: a brief overview of the genetic revolution," (in eng), *The Journal of the Association of Physicians of India*, vol. 61, no. 2, pp. 127-33, Feb 2013.

[7] A. Rodriguez, A. Del, and M. Angeles, "Non-Viral Delivery Systems in Gene Therapy," InTech, 2013.

[8] E. Yaniz-Galende and R. J. Hajjar, "16 - Stem cell and gene therapy for cardiac regeneration," in *Cardiac Regeneration and Repair*, R.-K. Li and R. D. Weisel Eds.: Woodhead Publishing, 2014, pp. 347-379.

[9] M. Ramamoorth and A. Narvekar, "Non viral vectors in gene therapy- an overview," (in eng), *Journal of clinical and diagnostic research : JCDR*, vol. 9, no. 1, pp. Ge01-6, Jan 2015, doi: 10.7860/jcdr/2015/10443.5394.

[10] A. Bolhassani, A. Khavari, and Z. Oraf, "Electroporation – Advantages and Drawbacks for Delivery of Drug, Gene and Vaccine," InTech, 2014.

[11] C. Faurie, M. Golzio, E. Phez, J. Teissié, and M. P. Rols, "Electric Field-Induced Cell Membrane Permeabilization and Gene Transfer: Theory and Experiments," *Engineering in Life Sciences*, vol. 5, no. 2, pp. 179-186, 2005, doi: 10.1002/elsc.200420068.

[12] A. Daemi, A. Bolhassani, S. Rafati, F. Zahedifard, S. Hosseinzadeh, and F. Doustdari, "Different domains of glycoprotein 96 influence HPV16 E7 DNA vaccine potency via electroporation mediated delivery in tumor mice model," (in eng), *Immunology letters*, vol. 148, no. 2, pp. 117-25, Dec 17 2012, doi: 10.1016/j.imlet.2012.10.003.

[13] A. Monie, S.-W. D. Tsen, C.-F. Hung, and T. C. Wu, "Therapeutic HPV DNA vaccines," *Expert Review of Vaccines*, vol. 8, no. 9, pp. 1221-1235, 2009, doi: 10.1586/erv.09.76.

[14] B. Rubinsky, "Irreversible Electroporation in Medicine," vol. 6, no. 4, pp. 255-259, 2007, doi: 10.1177/153303460700600401.

[15] T. Kotnik, "Transmembrane Voltage Induced by Applied Electric Fields," Springer International Publishing, 2017, pp. 1111-1127.

[16] P. Shi, N. Zhao, J. Coyne, and Y. Wang, "DNA-templated synthesis of biomimetic cell wall for nanoencapsulation and protection of mammalian cells," *Nature Communications*, vol. 10, no. 1, 2019, doi: 10.1038/s41467-019-10231-y.

[17] M.-P. Rols, "Gene Delivery by Electroporation In Vitro: Mechanisms," Springer International Publishing, 2017, pp. 387-401.

[18] L. Raptis and K. L. Firth, "Electrode assemblies used for electroporation of cultured cells," (in eng), *Methods in molecular biology (Clifton, N.J.)*, vol. 423, pp. 61-76, 2008, doi: 10.1007/978-1-59745-194-9_4.

[19] Q. A. Zheng and D. C. Chang, "High-efficiency gene transfection by in situ electroporation of cultured cells," (in eng), *Biochimica et biophysica acta*, vol. 1088, no. 1, pp. 104-10, Jan 17 1991, doi: 10.1016/0167-4781(91)90158-i.

[20] T. García-Sánchez *et al.*, "Design and implementation of a microelectrode assembly for use on noncontact in situ electroporation of adherent cells," (in eng), *J Membr Biol*, vol. 245, no. 10, pp. 617-624, 2012/10// 2012, doi: 10.1007/s00232-012-9474-y.

[21] Y. Xu, S. Su, C. Zhou, Y. Lu, and W. Xing, "Cell electroporation with a three-dimensional microelectrode array on a printed circuit board," (in eng), *Bioelectrochemistry (Amsterdam, Netherlands),* vol. 102, pp. 35-41, Apr 2015, doi: 10.1016/j.bioelechem.2014.10.002.

[22] Y. C. Lin, M. Li, and C. C. Wu, "Simulation and experimental demonstration of the electric field assisted electroporation microchip for in vitro gene delivery enhancement," (in eng), *Lab on a chip,* vol. 4, no. 2, pp. 104-8, Apr 2004, doi: 10.1039/b312804k.

[23] K. S. Huang, Y. C. Lin, C. C. Su, and C. S. Fang, "Enhancement of an electroporation system for gene delivery using electrophoresis with a planar electrode," (in eng), *Lab on a chip,* vol. 7, no. 1, pp. 86-92, Jan 2007, doi: 10.1039/b613753a.

[24] T. Jain and J. Muthuswamy, "Bio-chip for spatially controlled transfection of nucleic acid payloads into cells in a culture," (in eng), *Lab on a chip,* vol. 7, no. 8, pp. 1004-11, Aug 2007, doi: 10.1039/b707479d.

[25] H. Huang *et al.*, "An efficient and high-throughput electroporation microchip applicable for siRNA delivery," *Lab on a chip,* vol. 11, no. 1, pp. 163-172, 2011, doi: 10.1039/c0lc00195c.

[26] M. B. Fox *et al.*, "Electroporation of cells in microfluidic devices: a review," *Analytical and Bioanalytical Chemistry,* vol. 385, no. 3, pp. 474-485, 2006, doi: 10.1007/s00216-006-0327-3.

[27] J. Selvakumaran, M. P. Hughes, J. L. Keddie, and D. J. Ewins, "Assessing biocompatibility of materials for implantable microelectrodes using cytotoxicity and protein adsorption studies," IEEE, doi: 10.1109/mmb.2002.1002326. [Online]. Available: https://dx.doi.org/10.1109/mmb.2002.1002326

[28] H. Askari, H. Fallah, M. Askari, and Mehdi, "Electrical and optical properties of ITO thin films prepared by DC magnetron sputtering for low-emitting coatings," *arXiv pre-print server,* 2014-09-18 2014, doi: None arxiv:1409.5293v1.

[29] S.-L. Tran, A. Puhar, M. Ngo-Camus, and N. Ramarao, "Trypan Blue Dye Enters Viable Cells Incubated with the Pore-Forming Toxin HlyII of Bacillus cereus," *PLoS ONE,* vol. 6, no. 9, p. e22876, 2011, doi: 10.1371/journal.pone.0022876.

[30] R. Jaeger, *Introduction to Microelectronics Fabrication,* Second ed. (no. Modular Series on Solid State Devices),. Chapter 4 Diffusion, pp 88

[31] W. Strober, "Trypan Blue Exclusion Test of Cell Viability," *Current Protocols in Immunology*, vol. 111, no. 1, 2015, doi: 10.1002/0471142735.ima03bs111.

[32] MicroChemicals, "AZ 1500 Series.", "58014 F20-00 WNT Autumn Mystery".

[33] L. Hao, X. Diao, H. Xu, B. Gu, and T. Wang, "Thickness dependence of structural, electrical and optical properties of indium tin oxide (ITO) films deposited on PET substrates," *Applied Surface Science*, vol. 254, no. 11, pp. 3504-3508, 2008, doi: 10.1016/j.apsusc.2007.11.063.

[34] R. J. Connolly, G. A. Lopez, A. M. Hoff, and M. J. Jaroszeski, "Characterization of plasma mediated molecular delivery to cells in vitro," *International Journal of Pharmaceutics*, vol. 389, no. 1-2, pp. 53-57, 2010, doi: 10.1016/j.ijpharm.2010.01.016.

[35] M.A. Skinner, “The Combined Effect of Heat and Corona Charge on Molecular Delivery to a T-cell Line In-vitro”, M.S. Thesis, Biomedical Engineering, College of Engineering, University of South Florida, 2019.

Appendix A: Permissions

Non-Viral Delivery Systems in Gene Therapy

Alicia Rodríguez Gascón,
Ana del Pozo-Rodríguez and María Ángeles Solinís

Additional information is available at the end of the chapter

http://dx.doi.org/10.5772/52704

1. Introduction

Recent advances in molecular biology combined with the culmination of the Human Genome Project [1] have provided a genetic understanding of cellular processes and disease pathogenesis; numerous genes involved in disease and cellular processes have been identified as targets for therapeutic approaches. In addition, the development of high-throughput screening techniques (e.g., cDNA microarrays, differential display and database meaning) may drastically increase the rate at which these targets are identified [2,3]. Over the past years there has been a remarkable expansion of both the number of human genes directly associated with disease states and the number of vector systems available to express those genes for therapeutic purposes. However, the development of novel therapeutic strategies using these targets is dependent on the ability to manipulate the expression of these target genes in the desired cell population. In this chapter we explain the concept and aim of gene therapy, the different gene delivery systems and therapeutic strategies, how genes are delivered and how they reach the target.

2. Aim and concept of gene therapy with non-viral vectors

A gene therapy medicinal product is a biological product which has the following characteristics: (a) it contains an active substance which contains or consists of a recombinant nucleic acid used in administered to human beings with a view to regulating, repairing, replacing, adding or deleting a genetic sequence; (b) its therapeutic, prophylactic or diagnostic effect relates directly to the recombinant nucleic acid sequence it contains, or to the product of genetic expression of this sequence [4].

Figure1A: Permission for chapter 3.